A MOLECULAR DYNAMICS STUDY OF MECHANICAL PROPERTIES OF CARBON NANOTUBE POLYMER COMPOSITES AND GRAPHENE NANOPLATELET POLYMER COMPOSITES

A Thesis
Submitted to the Graduate Faculty
of the
North Dakota State University
of Agriculture and Applied Science

By

Suchitra Reddy Yerramaddu

In Partial Fulfillment of the Requirements
for the Degree of
MASTER OF SCIENCE

Major Department:
Mechanical Engineering

November 2010

Fargo, North Dakota

North Dakota State University
Graduate School

Title

A Molecular Dynamics Study of Mechanical Properties of Carbon Nanotube Polymer Composites and Graphene Nanoplatelet Polymer Composites

By

Suchitra Reddy Yerramaddu

The Supervisory Committee certifies that this ***disquisition*** complies with North Dakota State University's regulations and meets the accepted standards for the degree of

MASTER OF SCIENCE

SUPERVISORY COMMITTEE:

ABSTRACT

Yerramaddu, Suchitra Reddy, M.S., Department of Mechanical Engineering, College of Engineering and Architecture, North Dakota State University, November 2010. A Molecular Dynamics Study of Mechanical Properties of Carbon Nanotube Polymer Composites and Graphene Nanoplatelet Polymer Composites. Major Professor: Dr. Ghodrat Karami.

Carbon nanotubes have been the main focus in science and engineering fields lately for their extraordinary properties. But carbon nanotube fabrication process is very expensive, particularly for reinforcements and structural composite applications. Instead of working towards developing lower cost nanotubes, an alternate solution to resolve the problem is to formulate a cost effective reinforcement referred to as graphene nanoplatelets. These nanoplatelets have excellent mechanical as well as electronic properties opening up for several applications in various fields. Their structure with carbon-carbon bonds make them stronger and stiffer. Single nanotubes can be used as reinforcements in one direction, while the graphite nanoplatelets are effective in two directions yielding a higher degree of stiffness and strength in a matrix.

In this thesis, a molecular dynamic computer simulation technique was used to explore the atomic scale and dynamics of graphene nanoplatelets and carbon nanotubes embedded in polyethylene matrix. The mechanical properties of the carbon nanotubes and nanoplatelets polymer composite models were studied individually along with a comparison between composite models. The overall system was modeled using *material studio* software with the implementation of periodic boundary conditions to determine the properties. The stress strain curves revealed that the length and the volume fraction of the nanotube/nanoplatelets had a significant effect on the mechanical properties of the composite. The stiffness of the composite with long reinforcement length increased relative

to the polymer in the longitudinal direction and shows an anisotropic behavior. Significant enhancement was observed in the Young's modulus with the increase in the volume fraction of the nanotubes/nanoplatelets because of the well known effect of the increase in the load transfer between the polymer and the reinforcements. Also increasing the volume fraction of the short nanotubes/nanoplatelets provided very little improvement in stiffness compared to the longer length nanotubes/nanoplatelets. Results also showed that the graphene nanoplatelet reinforced composite properties were very comparable to the nanotubes reinforced composites even under weak vander Waal interactions.

ACKNOWLEDGEMENTS

I would like to thank my adviser, Dr. Ghodrat Karami, for his help, guidance and suggestions for the successful completion of my thesis. I would also like to thank Dr. Josh Wong for providing me the opportunity to work on the project and his support is greatly appreciated. Financial support for this work has been provided by the National Science Foundation.

I would also like to acknowledge my committee members, Dr. Alan Kallmeyer, Dr. Xinnan Wang and Dr. Dean Webster for participating in this research as committee members. In addition, I thank the faculty and staff of Mechanical Engineering Department of North Dakota State University.

I would especially like to thank my husband and my parents for all their support that allowed me to reach this level.

TABLE OF CONTENTS

TABLE OF CONTENTS (Continued)

LIST OF TABLES

LIST OF FIGURES

LIST OF FIGURES (Continued)

CHAPTER 1. INTRODUCTION

In recent years with the advancement of material synthesis and characterization on an atomic scale, wide spread interests have risen for nano sized materials. Carbon compounds have been the main focus for many industries from diverse fields. These compounds exhibit low mass to strength ratio which attracts the industries, who have been investigating cost effective new materials with similar properties. Studies have shown that nanofillers have exhibited excellent mechanical properties and have enhanced the polymer properties when embedded as reinforcements. Compared to the conventional fiber reinforced and non-reinforced polymers the nanocomposites possess some unique features and functions that make them standout. Their strength, modulus and dimensional stability significantly improve the mechanical properties of nanocomposite. Their small size facilitates in composite processing allowing molding the structure into unique shapes without losing the properties which is a huge advantage in manufacturing industry. The key to nanocomposite technology lies in nanoscale phenomena that revolutionize the engineering design of materials. Nanocomposites promote synergisms in structural integrity, functionality, versatility and cost effective fabrication. In recent years, carbon nanotube polymer composites have attracted a lot of attention because of their extraordinary structure which help improve the mechanical and physical properties.

Graphene has been studied by researchers lately as nano-reinforcement in various polymers. They have excellent stiffness, electrical and thermal conductivity which makes it an ideal reinforcement. A small addition can lead to significant improvements in matrix properties. They have been used in several applications including fuel tank and fuel line

coating where graphene nanoplatelets unique shape and size impart high barrier properties coupled with electrical conductivity, coating and paints, fuel cells and batteries for energy storage, RFI shielding in aerospace applications and in many automotive parts.

Many techniques exist and have been used to study the properties of nanocomposites. Computational approaches can play a key role in the characterization of the properties of the nanocomposites. Molecular Dynamics is one of the modeling techniques used to study the equilibrium and non-equilibrium molecular systems at a much lower cost and time compared to the experimental tests. This research focuses on the possibility of using graphene nanoplatelets in comparison to carbon nanotubes as reinforcements in a polymer matrix focusing on the mechanical properties of composites using molecular dynamic (MD) simulations. Literature reviews on various types of carbon compounds and the research conducted on molecular dynamic simulations will be discussed which provides a stage for modeling and analyzing the composites. The theory behind the molecular dynamics simulations, different force fields, and ensembles step wise details will be reviewed. Details of the nanocomposite structure building using the material studio software will be presented along with some of the challenges involved in nanocomposite design. The effect of the reinforcement type, length and the volume fraction on the polymer properties under longitudinal and transverse strain are discussed in detail with a comparison of the composite properties.

CHAPTER 2. LITERATURE REVIEW

Carbon and its Allotropes

Carbon is one of the few elements which are well known since antiquity. It is among those elements which exist in many different forms; notable forms include graphite and diamond. Graphite is considered as the only stable allotrope of carbon and diamond shows a slow behavior in changing into graphite at all temperatures. Carbon and its allotropic forms are used in several industrial, chemical and medical fields for the excellent mechanical and thermal properties. Another form of carbon called fullerenes are molecules composed entirely of carbon which exist in tubes, hollow spheres which are now referred to as buckyballs, nanofibers, nanobuds, nanofoams and nanotubes [1]. Figure 2.1 shows the different allotropic forms of carbon.

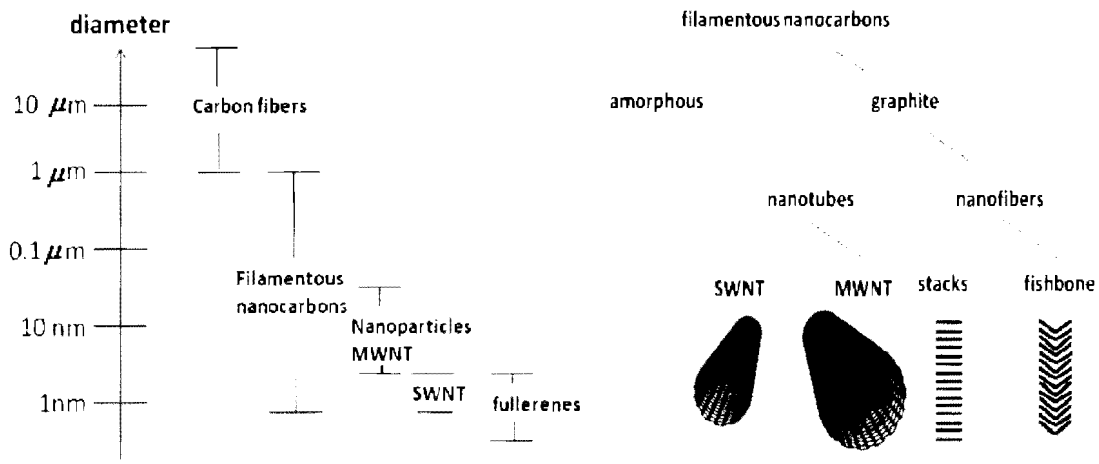

Figure 2.1 Carbon and its allotropic forms [2].

Effect of Size on the Strength of Materials

Griffith [13] in his study stated that the strength of the glass fiber depends on the size, the smaller the fiber the stronger it becomes and this theory has been confirmed by many researchers. He proposed that weakness of larger material is due to the increase in the defects such as cracks. He assumed that the work on creating new crack surface is equal to the strain energy released or the total amount of relaxation of material upon crack propagation. If the energy required for creating new crack surface is larger than the strain energy that would be released, the crack doesn't grow [4].

Based on his assumptions, Griffith proposed the existence of critical crack length at any given stress condition on a material. Griffith [5] crack length is described as follows

$$\sigma = \left(\frac{2E\gamma_s}{\pi a} \right)^{1/2} \tag{1}$$

Where, σ is the applied stress, E is the Young's modulus, γ is the surface tension and a is half of the crack length. Material failure will occur if the cracks are longer than this length. If the material is smaller than the critical crack length, it will not fail and reach its theoretical maximum strength.

Theories show that the smaller size materials can be stronger than the large ones and could be effective reinforcements if appropriate surface conditions are applied. Also materials with smaller size and high aspect ratios provide significant improvement in properties like thermal & electrical conductivities [4].

Background of Nanoscale Reinforcements in Composites

While many researchers have focused on clay platelets reinforced nanocomposite structures, similar concept applies to the graphite reinforced composites. Graphite is one of

the stiffest materials found in nature that has excellent electrical, thermal and mechanical properties [7]. It is a sheet like structure with atoms in the same plane. The covalent bonding between the carbon atoms makes it the strongest among the well known two dimensional structures. Compared to clay materials, graphite has better mechanical, electrical and thermal properties [6, 7]. The material characteristics are tabulated and shown in Table 2.1. For a long time, carbon and graphite materials have been used as fillers. One of the widely used carbon material as a filler is carbon black for its cost effectiveness. This material provides improved compound processability and useful properties such as ultraviolet, thermal protection and electrical conductivity. But, because of its poor mechanical properties and insufficient interactions with the polymer, it is instead used as filler for coloring or opacifying polymers [8].

Table 2.1 Properties of clay and graphite [6, 7].

Material Characteristics	Clay	Graphite
Chemical Structure	SiO2, Al2O3, MgO, K20, Fe2O3	Carbon
Physical Structure	Layer	Layer
Interactions between layers	Hydrogen Bond Dipole -Dipole	$\pi - \pi$
Tensile Modulus	172 Gpa	1060 Gpa
Tensile Strength	0.3 - 0.9 Gpa	20 Gpa
Thermal Conductivity	6.7×10^{-3} W/cm K	30 W/cm K
Coefficient of Thermal Expansion	$8 - 16 \times 10^{-6/k}$	$-1 \times 10^{-6/K}$
Resistivity	$10^{10} - 10^{16}$ Ω cm	50×10^{-6} Ω cm
Density	2.75 - 3.00 g/cm^3	1.80 - 2.00 g/cm^3

In 1950's graphite whiskers were fabricated by applying DC arc discharging process to graphite electrode under high temperature and pressure [9]. The material showed excellent material properties but the difficulty in large scale production prevented it from

being used in commercial applications. Figure 2.2 shows the structure of different forms of carbon.

By the end of 1960's some carbon fibers were commercially available and used in military grade aerospace applications. There were constant improvements made to the properties and with a price decrease it found many applications such as automobiles, commercial jet planes and sporting goods, but missed the opportunity of using them in large scale applications because of the relatively high cost associated with the carbon fibers.

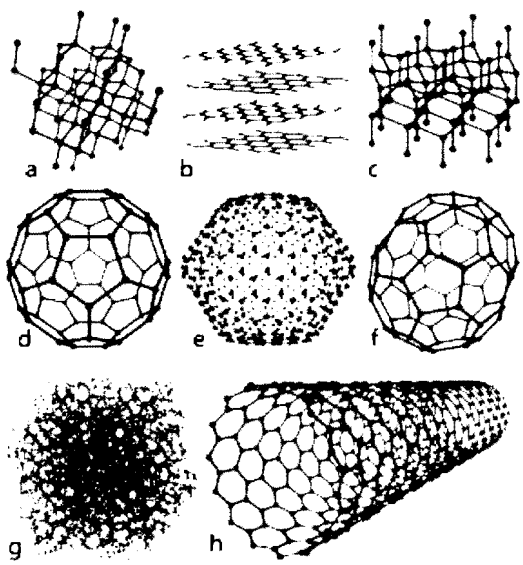

Figure 2.2 Allotropes of carbon (a) Diamond (b) Graphite (c) Lonsdaleite (d) Buckyball (e) C_{540} (f) C_{70} (g) Amorphous carbon (h) Carbon nanotube [10].

In 1985, a new structure of carbon material is found and named as fullerene or buckyball. It has a spherical shape, comprised of 60 carbons and they form five or six-membered rings like a soccer ball. These rings of carbon atoms can be bent into ellipses, cylinders or spheres. The carbon atoms folded into a cylindrical tubular shape are called

carbon nanotubes. The most common of them is the C_{60} bucky ball structure which was discovered by Robert Curl, Harold Kroto and Richard Smalley in 1985. The C_{60} resembles a soccer ball structure with pentagonal and hexagonal face composition. Among the fullerene structures discovered this has a high degree of symmetry [6]. They are very stable structures both physically and chemically because of the strong bonding between the atoms. During the discovery there was much excitement about the practical applications of these structures. Some of them include uses in organic photovoltaics, and being powerful antioxidants can be used in health and personal care applications. Bucky balls are used in wide range of applications. Their magnetic property with one unpaired electron makes it a potential candidate for magnetic resonance imaging along with applications in optical devices, energy storage and electro chemical applications [7, 8]. Currently research is being done to use them for novel drug delivery systems.

A new structure of carbon was reported in 1991 by Iijima [11], because of its size and tubular shape it is called carbon nanotube. Researchers predicted that the material has the highest available mechanical and electrical properties among the carbon materials, a lot of researches in a variety of fields are now working with this material. Carbon nanotubes extraordinary characteristics give them potential to be used in structural applications, antistatic coatings, energy storage, shielding and microelectronic applications [12]. But the lower productivity, ability to produce in large quantities and fabrication cost make it difficult to be used in large commercial applications. Crystalline graphite materials also have excellent mechanical and thermal properties and are much readily available. Even though carbon nanotubes possess better properties compared to the graphite materials, crystalline graphite are readily available and are much cheaper which make it a better

choice for commercial applications [13]. If proper surface treatments are applied to the layered graphite structure they can act as reinforcements for composites improving the mechanical, electrical and thermal properties. The material properties are illustrated in Table 2.2.

Table 2.2 Properties of carbon/graphite materials [14].

Material	Diameter (um)	Length (um)	Tensile Modulus (Gpa)	Tensile Strength (Gpa)	Thermal Conductivity (W/m K)	Electrical Resistivity (Ω cm)	Cost ($/lb)
Carbon Black	10-300	10-300				10^{-1} - 10^{2}	< 0.4
High Modulus Carbon Fiber	4.3-8.4	Continuous	400-800	2.5 - 4.0		1.7×10^{-3}	15 – 25
High Strength Carbon Fiber	4.5-7.2	Continuous	250-300	5 - 7		6.8×10^{-3}	< 15
Vapor Grown Carbon Fiber	0.1-10	10-500	250-500	3 - 7	20 – 3000	7×10^{-5} - 1×10^{-3}	40 – 50
Carbon Nanotube	0.007-0.1	1	1250 ~ 2000	50 ~ 180	3000		40000
Single Crystal Graphite	0.4-2000	thickness 0.005-100	1000	10-20	3000	5×10^{-5}	< 5

Carbon Nanotubes and their Mechanical Properties

Carbon nanotubes are thin nano threads made of pure carbon have been the object of intense scientific study since then [15, 16]. They are molecular scale graphitic carbon rolled into a tube. The CNT length ranges from a few tens of nanometers to several micrometers, and in outer diameter from about 3nm to 30 nm [17]. Figure 2.3 shows the diameter comparison of different carbon materials. They are extremely small in size having strengths 20 times that of high strength steel alloys, half as dense as aluminum and having

current carrying capacities with superior thermal properties compared to diamond. Two years later the single walled nanotubes were independently created with just one layer of carbon atoms. CNTs have been identified as one of the most promising building blocks for future development of molecular mechanics. Despite the potential impact that new composites based nanotubes would affect many areas of science and technology, a complete characterization of the material properties is still underway.

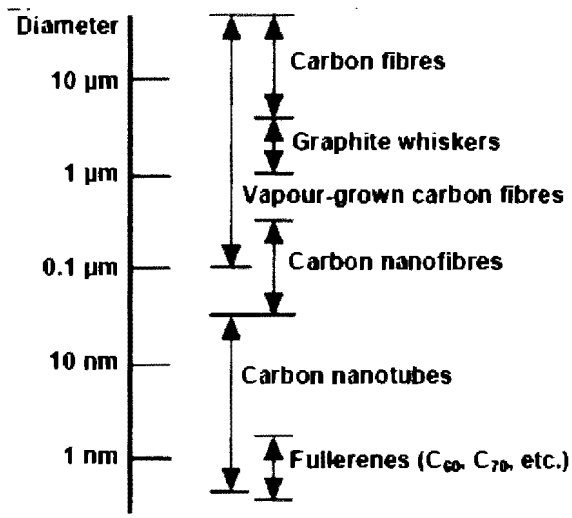

Figure 2.3 Diameter comparison of various carbon-based materials [18].

In general, CNTs are classified under two categories: Single Walled Carbon Nanotubes (SWNT), and Multi Walled Carbon Nanotubes (MWNT), Figure 2.4. A SWNT could be viewed as a conformal mapping of two dimensional honeycomb lattice i.e., a sheet of carbon atoms whose bonds form a hexagonal pattern. It is possible to roll at any angle with respect to the honeycomb structure and make the tube any diameter one can choose. These two parameters angle and diameter determine the specific type of CNT

being formed, and its properties depend sensitively on structural details such as tube radius and helicity. The MWNT can be thought of as two or more concentric shells of carbon sheets [19]. The CNTs can be sealed at both the ends using endcaps, generally called as hemispherical caps. If the endcaps are neglected the focus is on the large aspect ratio of the cylinder (i.e., length to diameter ratio) which is generally called as long/continuous CNTs.

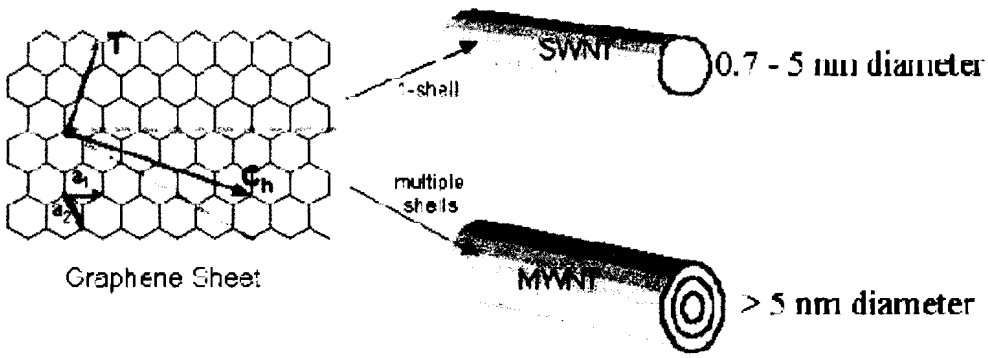

Figure 2.4 Graphene sheet rolled into SWNT and MWNT [20].

Various types of cylindrical shells are possible: armchair tubule, zigzag tubule and chiral tubule as shown in Figure 2.5. The nomenclature (n, m) of each tubule refers to integer indices corresponding to the chiral vector, Ch, along which the graphene sheet has been rolled. The nanotubes of type (n, n) are commonly known as armchair tubes while zigzag tubes correspond to the case where m=0, or Ch = (n, 0).

Another method of labeling these structures is based on the shapes made by the most direct continuous path of bonds around the circumference of the nanotube. Specifically, the (n, 0) type structures are labeled as saw tooth, and the (n, n) type structures as serpentine. For all other conformations in equivalent to these two sets, the nanotubes are referred to as chiral [22].

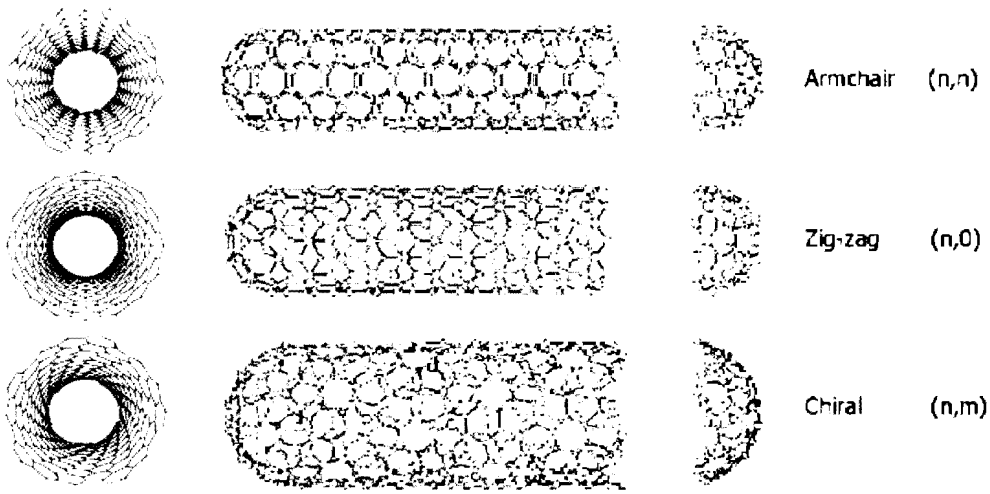

Figure 2.5 Classification of nanotubes: Armchair, Zig-zag and Chiral nanotubes [21].

Theoretical studies of these graphitic tubules have focused primarily on their electronic properties whereas relatively little has been reported regarding the mechanical properties of these exotic materials. Research showed that the SWNT possess extraordinary mechanical properties with the Young's modulus of 1 Terra Pascal and an estimated tensile strength of 30GPa which is as stiff as diamond. It is believed that the stiffness and strength of CNT is dependent on the diameter and structure of the tube. This is true for both the multi walled and single walled nanotubes, since the modulus is determined by the carbon bonds within the individual layers. Buckling rather than fracture is a common phenomena observed in nanotubes. It is observed that thicker wall tubes tend to get buckled while the thinner tend to collapse. It is estimated that the carbon nanotubes have compressive strengths at least 100 times greater than any other known fiber [23]. Research also illustrates that the mechanical properties of the CNTs is dependent on the diameter and their properties approach graphene with the increase in the diameter [15]. It has also been

found that a qualitative relationship exists between the Young's modulus of a CNT and the amount of disorder in the atomic structure of the walls [24]. Nanotube flexibility under mechanical loading plays important role for their application as nano-probes and in nano-composites. The mechanical properties of different types of nanotubes are summarized in Table 2.3.

Table 2.3 Mechanical properties comparison of different types of carbon nanotubes [25].

Material	Young's modulus (Tpa)	Tensile Strength(Gpa)	Elongation at break
SWNT	~ 1 (from 1 to 5)	13-53 (E)	16
Armchair SWNT	0.94 (T)	126.2 (T)	23.1
Zigzag SWNT	0.94 (T)	94.5 (T)	15.6-17.5
Chiral SWNT	0.92		
MWNT	0.8-0.9 E)	150	
Stainless Steel	~0.2	~0.65 -3	15-50
Kevlar	~0.15	~3.5	~2
T - Theoretical & E - Experimental			

Due to their incredible properties, size and function they have been researched for many materials and technologies. Their ideal usage in future is to modify the existing material properties creating the nanocomposite structures. Since CNTs are hollow, tubular, caged molecules they have been proposed as lightweight storing material for hydrogen and to be released for efficient fuel cells used in electric cars [17]. Their large surface area and electrical conductivity make them excellent candidates for electrochemical applications. Limitations include the fabrication cost, interfacial strength between the CNT/polymer and the CNTs dispersion. Methods to overcome the limitations are being researched.

Graphene Nanoplatelets

Graphene Nanoplatelet (GNP) material is distinctly different from the existing carbon black, CNT and smectite clay reinforcements in terms of its unique processing techniques for nanoscaled reinforcements, cost effectiveness and functionality. They have twice the surface area compared to CNT, their properties and features should make them outperform other nanomaterials that are available currently in the market. It is a thick sheet of graphite in a honey comb pattern and is treated as the unrolled form of CNT, sharing some of its unique properties. GNP is a two dimensional material with carbon atoms connected to each other through sp2 bonds and possess unique properties such as high strength, excellent thermal and electrical conductivities which makes them attractive for many applications. Strong covalent bonds exist in between the carbon atoms in the 2-D plane but the layers of graphene are connected through weak vander Wall forces as shown in Figure 2.6. The bond length of C-C bond in graphene is around 0.14nm.

The density in graphite in different media is tabulated in Table 2.4. Several methods have been used to prepare the GNPs or graphenes among which are the chemical intercalation-hot expansion ultrasonification method and chemical oxidation-in situ reduction ultrasonification method. These methods were able to develop graphite sheets with less than 10nm thickness. Typical GNP thickness can range from 0.34-100 nm. With a tensile strength of 130 GPa and a Young's modulus of 1 Tpa, graphene sheet is the strongest material existing [26].

GNPs play a significant role in nanoscale electronics as a conductor for wires and other elements, electrons can flow through the element at a very high speed without any collision with the atoms.

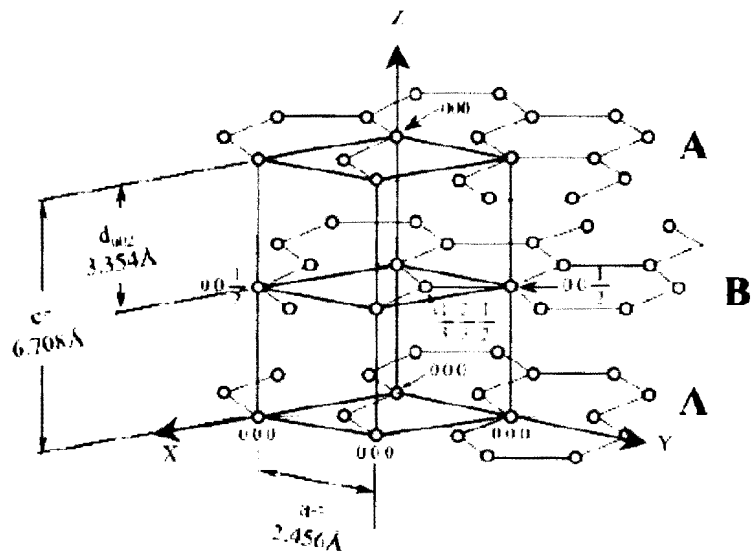

The structure of graphite, formed by the *AB* stacking of graphene sheets.

Figure 2.6 Structure of graphite with graphene sheets stacked up [24].

The dielectric property of a matrix is based on several factors including the volume of the fillers, shape and interactions between the reinforcement and the polymer. Dielectric property is defined as the ratio of electrical energy stored in a system during the application of potential relative to vacuum dielectric constant.

Research conducted by Zheng and Wong [28] showed that the nanocomposite with GNPs had much bigger loss factor when compared to the polymer PMMA. Low filler content was required for the nanocomposite which resembles much to semi conductors.With their high strength and modulus, GNPs enhance the mechanical properties of the matrix in multiple directions. But, improvement in tensile properties was only proved in some research while others contradict since there was no enhancement with the addition of the GNPs [29].

Table 2.4 Graphitic densities [27].

	Density(g/cm^3)	Immersion Media
Synthetic Graphite	2.091 2.093	n - hexane Helium
Oxidized Graphite	2.224	Methanol
Dust	2.220	Helium
Natural Ceylon	2.253	Methanol
99.50%	2.251	Helium
Pyrolytic	2.07 to 2.22	

Also, significant improvement was observed in the glass transition temperature with the addition of the nanofillers [30]. Their excellent properties and low cost indicates their potential to be used as reinforcements for improving mechanical, thermal and electrical properties of the polymers.

Literature Survey on Graphene Nanoplatelets

Although GNP and CNT are geometrically different, some initial studies have shown that they have similar mechanical and thermal properties. New patents and research findings continue to emerge with novel processing methods to produce highly expanded graphite [31]. Instead of developing the lower-cost process for fabrication of CNT, the use of natural flake graphite is being experimented, which exists abundantly in our planet earth, coupled with mechanical attrition processes to produce low-cost nanoscale substitutes that provide attractive functional properties when dispersed in polymer matrices [32]. It was in 1970 when the production of graphene nanosheets was first reported [33] and later in 2004

was when the single layer graphene was separated from graphite using a micromechanical cleavage method [34]. A lot of research is being done on the graphene nanoplatelets after the discovery of methods for their production. Graphene can be produced using methods such as arc discharge, chemical conversion, chemical vapor deposition and self assembly of surfactants but because of the large amount of graphene required for the polymer nanocomposites these methods are not suitable for this application [35]. Research has also shown that graphene produced through exfoliation of the graphite is much suitable for the polymer composite applications because of the capability to produce in large quantities. Direct Sonication is another method which can produce single and multi layered graphene in large quantities but exfoliated graphene sheet separation from the graphite is a challenge. Expanded graphite, commonly used as filler for the polymer composites is another form of carbon which is produced by heat treatment method. Some significant amount of work has been done in Drexel and Michigan State Universities [36] focusing on composites involving clay and graphite nanocomposites along with their patent on the method for producing the graphene platelets. It has been proven that GNP significantly improves the mechanical and electrical conductivity of the polymers compared to graphite at smaller loadings [37]. Dispersion of graphene in polymers strongly affects the properties of polymer composites. Some in-depth investigations have been done in the property profiles of graphene in comparison to established CNTs. Recently, Wong and collaborators examined the novel properties such as elastic, electrical and dielectric properties that could be derived from GNP-reinforced polymer nanocomposites [38]. In situ intercalative polymerization of monomers can produce graphene composites. Polymerization of several materials poly vinyl acetate (PVA), poly methyl methacrylate (PMMA) and epoxy with

graphite oxide and polyurethane with thermal expansion of graphite oxide have been reported by Jang et al [39]. The physical structure of the GNPs and its large surface area makes it an ideal case for reinforcements.

Graphene is the stiffest material ever reported and despite of some structural distortion the modulus is still as high as 0.25 TPa [40]. Ramanathan et al have reported the advantages of graphene over several other carbon fillers like carbon black and single walled carbon nanotube in their study [41]. Kim et al have compared the stiffness of different types of graphene and the results indicated that the increase in stiffness is determined by the length of the graphene layers rather than the aspect ratio of the sheet [42]. Odegard and Gates have recently been working on mechanical characterization of graphite epoxy nanocomposite using multi scale analysis [43]. A micro mechanical analysis approach was used to determine the mechanical properties of the GNP epoxy composite varying the volume fraction and the length of the platelets. The elastic constants calculated compared well with the experimental data and the results showed that the nanocomposite modulus was dependent on the aspect ratio of the reinforcements. GNP can serve as an alternative nano reinforcement material with comparable properties like CNT and their composites can also be produced cost-effectively using scaled-up production routes.

Nanocomposite Applications

Nanocomposites have been in existence for a long period of time although it was after 1980s when these materials were main focus for research. Soon after these nanocomposites have gained popularity and have been an exciting field in material science.

There has been a great amount of studies being done investigating and exploiting these nanostructures. A nanocomposite is described as a matrix or composite where one of the phases one, two or three dimensional is on a nanometer size scale.

In the past decade, extensive research has focused on polymer nanocomposites in hopes of exploiting the unique properties of materials in the nano-sized regime [44]. A general conclusion has been drawn that nanocomposites show much improved mechanical properties over their micro-sized similar systems. Because of their small size, nanoparticles have a high surface to volume ratio and provide high energy surfaces. And embedding nano particles into the polymer matrix result in enhanced bonding between the polymer and filler from their high interfacial energy [45]. Polymer composite theory predicts that improved bonding between polymer and matrix leads to improved mechanical properties [46]. Nano reinforcements in polymer matrix provide several advantages, when dispersed in polymer their large surface area would cause polymer confinement leading to high strength and stiffness of the composite. They enhance the thermal and electrical conductivity, chemical resistance, flame retardancy and optical clarity.

Theoretically many models and theories have been proposed and developed to predict the modulus of the nanocomposites. The basic concept of theoretical estimation started with the rule of mixtures assuming the fibers are uniaxially aligned and perfectly bonded to the matrix considering both matrix and fibers are elastic and isotropic materials [47]. In 1950's Eshelby introduced a new model that had a single ellipsoidal inclusion embedded in an infinite medium which undergoes uniform deformation corresponding to impose deformation in the media at large distances from the inclusion. This model was able to predict elastic constants of composites with reinforcement of different shapes. But

research done by Shia and Hui contradict Eshelby's theory from their experimental data when the modulus of the reinforcement is much larger than the matrix [48].

Research done in the area of failure mechanisms of composites contains yielding of ductile materials, fracture of brittle materials and fatigue. This would apply for the thermoplastic and thermoset polymer materials. For short fiber reinforced polymer composites the fracture could be combination of multiple mechanisms based on the bonding between the matrix and the fibers. And research has shown that the failures get initiated by interfacial debonding around the reinforcements [49]. The fracture toughness of composite materials could increase, remain constant, or decrease with increasing reinforcement content as a result of a complex combination of many mechanisms. Composite strength is dependent on the adhesion condition and stress concentration at the interface. The bond leads to a good stress transfer from matrix to reinforcements which would lead to a higher strength. The stress at the interface can be affected by the shape, aspect ratio and the dispersion or arrangement of the reinforcements in the matrix [50]. So the composite materials can show higher toughness with lower strength [51]. Thus it is especially important to improve the adhesion for the overall mechanical properties of the system.

Literature Survey on Molecular Modeling of Carbon Nanotubes

In recent years, widespread interests have been risen for modeling of systems such as single-walled carbon nanotube (SWNT) and clay reinforced polymer composites. The advantages of predictive models are the following: (1) it establishes the feasibility for pilot fabrication of actual composite systems; (2) it provides guidance for experimentalists to

design the micro-nano-structures of the composites to obtain optimal properties without resorting to the trial and error approach; and (3) models and examines the interfacial bonding and adhesion at nanoscale whereby experiments are difficult to formulate. At nanoscale, it becomes tedious task to solve the analytical models and also the experimental tests are very expensive to be conducted. However modeling and simulations of nanocomposites can be cost effectively achieved using the computational approaches on a computer. Molecular dynamic simulation is one of tool proven to characterize and understand the CNT polymer composites properties and their interactions. Enough research has been done to understand the molecular dynamic (MD) approach to nanofillers and nanofiller reinforced composites [53]. Literature proves that MD simulations have been a reliable tool for understanding the atomic behavior, nanofiller and polymer interactions and load transfers.

Many researchers have been focusing on the composite modeling with CNTs as reinforcements. Feng and Huang have used nano mechanic approach for studying the CNT polymer composites and have discussed the bonding interactions between the polymer and the CNT and the effect of load transfer on the stiffness of the composites [52]. Griebel and Hamaekers have performed the molecular dynamic simulation over the polymer-CNT composite to study the elastic moduli of the composite from the stress strain curves [53]. They also concluded that the longer nanotubes provide better stiffness to the composite along with the alignment of the nanotubes parallel with the loading direction using the Parrinello Rahman approach. Also, the results from the MD simulation were compared to the rule of mixtures method. The research related to the introduction of chemical cross links between the polymer and CNT and its effect on the shear strength of interface was

done by Frankland et al [54] discussing the increase in the strength and modulus with the introduction of chemical bonds between the CNT and polymer. Wang et al [55] have conducted study on the modeling of polyethylene and functionalized CNT composites and found that the different degrees of functionalization affect the structure of the matrix if nanotube volume is less than 50%. Odegard et al research on the constitutive modeling of nanotube-reinforced polymer composites provided evidence that the length and volume fraction of the nanotubes does have an effect on the modulus of the composite using the equivalent continuum modeling approach [56]. Elastic properties of polymer carbon nanotube composites using molecular dynamic simulations was done by Han and Elliott and results support the idea that the addition of carbon nanotubes mechanically reinforce the polymer properties particularly in the longitudinal direction of the nanotube [57]. Coleman and Cadek study on poly vinyl alcohol showed a significant increase in Young's modulus with the addition of CNTs. In their comparison study of reinforcements the composites with CNTs showed the highest increase in modulus compared to others [58]. Tallury and Pasquinelli work on the molecular dynamic simulations of flexible polymer chains wrapping around the single walled carbon nanotubes indicated that the polymer with flexible backbones tend to wrap around the nanotube, but polyacrylonitrile with cyano group tends to transverse through the length of the nanotube rather than wrapping around the tube [59]. Using molecular dynamic simulations Li et al [60] measured the interfacial sliding of the carbon nanotube embedded in a diamond matrix. Their research indicated that the vander Waals interaction and sp3 bonding had a significant influence on the friction at the nano-scale. Ruoff et al research resulted in the process of producing the highly oriented pyrolytic graphite (HOPG) and their manufacturing. In their study they also

discussed the properties of the graphene sheet and their potential to be used as reinforcements [61]. This research uses the MD simulations approach to study the mechanical properties of both CNT & GNP composites considering vander Waals interactions between the reinforcement and the polymer with a report on the comparison data.

CHAPTER 3. MOLECULAR SIMULATIONS

Introduction to Molecular Simulations

With the growing interest in nanotechnology field, several nanometer size devices are being developed for various applications. This would require physical approaches for predicting its design and performance which is time consuming and expensive. This is where modeling and simulation play a key role in comparison to reduce the product development cost and time [62].

Molecular simulations in general can be used to compare the experimental results of an element to the calculated properties. It will be a great benefit to utilize the molecular simulations for studying a system which is still in the development phase and has not been researched using experiments to provide guidance for future work. This would require a robust simulation system with enhanced functional parameters which can be improved by validating the simulations in comparison to the experimental study. Improvements in the forcefields, studying the molecular interactions would lead to molecular simulations guiding the physical experiments which then can be used to study the properties such as Young's modulus, strength, thermal expansion, specific heat etc. Molecular dynamic simulation is one of the techniques in molecular simulation work [63].

Theory of Molecular Dynamic Simulations

Alder and Wainwright were the first people to introduce molecular dynamics to study the condensed fluid phase and later Rahman introduced the Lennard Jones potential for studying the long range interactions in liquid argon. Since then, MD simulations have

been widely used for studying the bulk properties of systems and understanding some complex systems [64, 65].

The theory behind the modeling is to relate the atomic trajectories to the macroscopic properties of the system. So at an atomic level studying the structure and dynamics would dictate the bulk properties of a system at macroscopic level. MD is a technique for following the progression of a system of atoms or molecules through phase space. From a given set of initial conditions and interatomic potentials, one can generate the trajectories for particles which are used to determine the physical properties.

All simulations in this study were performed with a commercial molecular simulation package Materials Studio (Discover) from Accelrys Inc. Discover has the ability to study molecular systems and a variety of material types. It incorporates a range of well validated potentials for dynamic simulations, minimization and conformational searches. The procedure involves setting up the system, minimizing the system using methods and algorithms, running the dynamic simulation under different conditions using a range of ensembles and analyzing the trajectory generated by one or more simulation.

A key assumption in MD is that the movement of atoms can be treated using classical mechanics. If the equation of motion holds, then the same equations of motion that govern macroscopic objects may be used to model the trajectories of atoms or molecules.

In fact, the motion of all but the lightest of atoms can be treated accurately by classical mechanics even though the interactions between atoms, which are a product of the motion of electrons, must be calculated using quantum mechanics. Luckily, the mass of nuclei is on the order of ten thousand times than of an electron. The position of the electron is highly localized due to its high velocities and low mass and has a short relaxation time.

In contrast, the heavier nucleus has a highly localized position and requires much more time to reach its equilibrium state than the electrons encircling it. The two motions can therefore be decoupled and treated independently. This is known as Born-Oppenheimer Principle. The energy of a given configuration of atoms can be calculated using Quantum Mechanical theory [66]. By varying the distance between the atoms, the potential energy as a function of configuration can be developed and the motion of large system of atoms can be calculated without explicitly taking the electrons into account. The time development of a many particle system is derived by numerically integrating the Newton's equation of motion generating a trajectory specifying the positions and velocities of particles varying with time. In the simplest form, Newton's equations of motion are solved:

$$F_i = m_i \times a_i \tag{2}$$

Where F_i is the force, m_i is the mass of atom, and a_i is the acceleration.

The force on an atom is a function of atomic coordinates in a system and so the equations of motion are solved with respect to time, since the positions and velocities of the atoms change. And so the force on an atom is obtained from the derivative of the potential energy with respect to the atom coordinates.

$$-\frac{dE}{dr} = m\frac{d^2r}{dt^2} \tag{3}$$

Where E is the potential energy of the system, m is the mass of the atom and r is the atom coordinates. The atoms are initially assigned velocities which are dependent on the simulation temperature and then once the forces are known the accelerations of the atoms in the system can be determined. The equations when solved yield a trajectory which describes the atom coordinates and velocities with respect to time. The method is

deterministic, once the positions, velocities of an atom are known; the state of system at a later time can be predicted. Finite difference method is typically used to solve the differential equations and in generating the trajectory file. Many algorithms have been developed for solving the equations of motion; the most popular is the Verlet velocity integrator because it requires moderate memory and is relatively fast [67]. The Verlet velocity algorithm is as follows:

$$r(t+\partial t) = r(t) + \partial t v(t) + \frac{\partial t^2 a(t)}{2} \tag{4}$$

$$a(t+\partial t) = \frac{f(t+\partial t)}{m} \tag{5}$$

$$v(t+\partial t) = v(t) + \frac{1}{2}\partial(t)[a(t) + a(t+\partial t)] \tag{6}$$

Where r is the position, v is the velocity, a is the acceleration of a given atom at time t. Mostly the selection of the algorithm is based on the type of simulation to be performed.

Force Fields and Parameters

Interactions between different types of atoms in MD are studied through the forcefield. The purpose of the forcefield is to describe the potential energy surface of the entire class of molecules with reasonable accuracy. There are many types of forcefields that exist but using the appropriate forcefield and its quality with its ability to predict the properties determines the validity. Forcefield used in molecular modeling involves forces derived from bond stretching, angle bending, bond rotations including non-bonded interactions to describe the vander Waals and electrostatic interactions between the atoms. All these parameters when combined with the functional form of energy terms are described as a forcefield. In this study polymer consistent forcefield (PCFF) is used which

is intended for polymers and organic material applications. The PCFF forcefield has been parameterized, tested and validated for calculating the thermal and mechanical properties with good accuracy [68].

The total potential energy of the model is described as a combination of the atomic coordinates with the force field information. It is sum of bonded and non-bonded interactions. The energy of bonded and non bonded interactions in a forcefield accounts for bond stretching, angle bending, electrostatic and vander Waal terms. The forcefield is broken down in following terms:

$$E_{total} = E_{bonded} + E_{non-bonded} \tag{7}$$

$$E_{bonded} = E_{bond-stretch} + E_{angle-bend} + E_{torsion} + E_{coupling} + E_{outofplane} \tag{8}$$

$$E_{non-bonded} = E_{vdw} + E_{coulomb} \tag{9}$$

$$E_{bond-stretch} = \sum_{b}\left[K_b(b-b_o)^2 + K_b(b-b_0)^3 + K_b(b-b_0)^4\right] \tag{10}$$

$$E_{angle-bend} = \sum_{\theta}\left[K_\theta(\theta-\theta_0)^2 + K_\theta(\theta-\theta_0)^3 + K_\theta(\theta-\theta_0)^4\right] \tag{11}$$

$$E_{torsion} = \sum_{\phi}\left[K_\phi(1-\cos\phi) + K_\phi(1-\cos 2\phi) + K_\phi(1-\cos 3\phi)\right] \tag{12}$$

$$E_{coupling} = \sum_{b}\sum_{b'} K_{bb'}(b-b_0)(b'-b_0') + \sum_{\theta}\sum_{\theta} K_{\theta\theta'}(\theta-\theta_0)(\theta'-\theta_0')$$

$$+ \sum_{b}\sum_{\theta} K_{b\theta}(b-b_0)(\theta-\theta_0)$$

$$+ \sum_{b}\sum_{\phi} K_{b\phi}(b-b_0)[F_{b\phi}\cos\phi + F_{b\phi}\cos 2\phi + F_{b\phi}\cos 3\phi]$$

$$+\sum_{\theta}\sum_{\phi} K_{\theta\phi}(\theta-\theta_0)[F_{\theta\phi}\cos\phi + F_{\theta\phi}\cos 2\phi + F_{\theta\phi}\cos 3\phi]$$
$$+\sum_{\theta}\sum_{\theta}\sum_{\phi}(\theta-\theta_0)(\theta'-\theta_0')(\phi-\phi_0)$$

(13)

$$E_{outofplane} = \sum_{x} K_x x^2 \tag{14}$$

$$E_{vdw} = \sum_{ij} \varepsilon_{ij}\left[\left(\frac{\sigma}{r}\right)^{12} - \left(\frac{\sigma}{r}\right)^{6}\right] \tag{15}$$

$$E_{coulomb} = \sum_{ij} \frac{q_i q_j}{r_{ij}} \tag{16}$$

Where $\boldsymbol{K}$ is the forcefield parameter, b is bond length between atoms, b_0 is the reference bond length at minimum energy state, θ is the bond angle, θ_0 is the reference bond angle, ϕ is the torsion angle, σ is the Lennard-Jones length parameter, x is the out of plane coordinate, $q_i q_j$ are the atomic charge of atom i and j, r_{ij} is the distance between atoms i and j and ε_{ij} is the vander Waal minimum interaction energy [69].

All the parameters and constants required to calculate the potential energy are stored in a file which will be referred during the simulation run. Each atom before running the simulation is assigned a forcefield type and the assignment is truly based on the atom type and properties. The accuracy of the results from a simulation greatly depends upon the type of forcefield [70]. The energy calculations depend significantly on the size of the structure meaning the number of atoms. With a large number of atoms the calculations get computationally long and expensive and so to reduce the efforts a cut off distance is assigned to the non-bonded interactions. The energy calculations only happen until the specified distance and the interactions beyond are ignored.

When running a simulation, time step is a very critical factor that needs to be considered. If during the MD simulation the time step specified is too large it would result in high energy overlapping between the atoms and would create instabilities and if small would not cover the complete phase space with inaccurate results. Reference guidelines exist in literature for different motion types for choosing the time step which is illustrated in Table 3.1.

Table 3.1 Guidelines for choosing time step for different motion types [71].

Atoms	Translation	10^{-14}
Rigid Molecules	Translation & Rotation	5×10^{-15}
Flexible molecules, rigid bonds	Translation, Rotation & Torsion	2×10^{-15}
Flexible molecules with flexible bonds	Translation, Rotation, Torsion & Vibration	$10^{-15}-5\times10^{-16}$

Types of Ensembles

Simulation ensemble is another important factor in MD study. If the above equations produce a trajectory with a constant number of particles (N) and volume (V) the simulation is said be to be performed in microcanonical ensemble (NVE). Also, using the ensemble the temperature (T) and pressure (P) of a dynamic run can be controlled to simulate the exposure of a system to external pressure or the exchange of heat with the

environment [72]. NVE ensemble is traditionally used in the MD simulations, but depending on the system and requirements different ensembles can be chosen.

For conducting an ensemble with constant particles, volume and temperature (NVT) referred to as canonical ensemble; a heat bath is coupled to the equations of motion allowing the transfer of energy to and from the system. Several methods exist for using the ensemble; velocity scaling, iso-kinetic method and stochastic method [73]. During the use of periodic boundary conditions in the simulation if pressure does not act as an important factor coupling to the pressure bath will not be necessary leading to less noise in the trajectory.

The equations of motion can be similarly modified to ensemble with constant number of particles, pressure and temperature (NPT) where the volume is allowed to change similar to a system in thermodynamic equilibrium. Several methods have been developed to control the pressure in the ensemble. One of those methods is the Berenden and Anderson method [74] which would only change the size of the cell but the Parinello – Rehman approach which is most widely used can control the stress allowing both the cell size and shape to change. In this formulation, the coupling between motions of the simulation cell is assumed to be weakly coupled to the motion of the particles. NPT ensemble can also be used to reach to required temperature and pressure before running another ensemble during equilibrium [74]. Motion of the atoms gets restricted during high pressure which would slow down the process. It is also important to conserve energy for generating correct statistical ensembles.

Due to the computational constraints, the particle number in atomistic simulation is severely limited. Surface effects may negatively affect even the largest of simulations. In

order to reduce the surface effects, periodic boundary conditions were employed. This means that the simulations take place in a computational cell surrounded by infinite number of identical replica cells. Only the behavior of one cell, which is the central cell, is simulated and all other cells behave in a similar fashion. When the periodic boundary conditions are used some particles may cross the cell so for each particle leaving the cell at the same instant an identical particle from an adjacent cell enters the cell at the opposite side as shown in Figure 3.1.

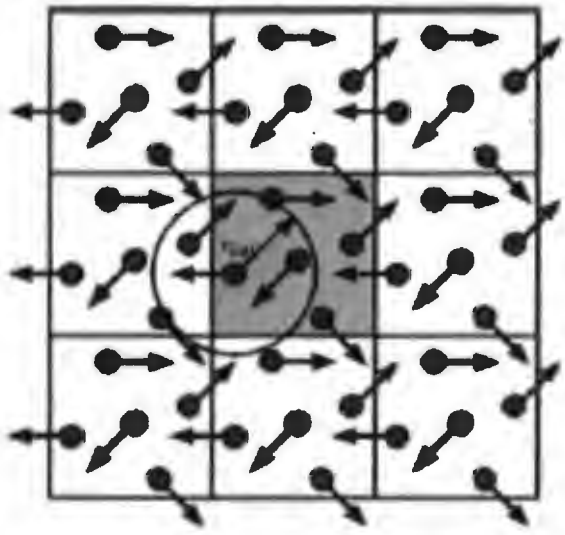

Figure 3.1 Periodic boundary condition in molecular dynamic simulation [75].

System Minimization

When a structure is created for simulation the molecules are always in high conformation and it is required to be optimized to a stable conformation to avoid erroneous results. This activity in MD is termed as minimization. It is a procedure where the atomic coordinates and the unit cell parameters are adjusted to bring the total energy of the system

to a minimum. It results in a structural model, which closely resembles the experimentally observed structure. Different minimization methods can be used to provide a static description of a molecule or system [76]. The minimization dialog allows you to set the minimization method, specify the convergence level and the number of interactions.

There are several minimization methods available which include the derivative minimizations and non-derivative minimization methods. Derivative minimizations use energy derivatives with respect to the atomic coordinates are useful because they provide information about the shape of the energy surface, and, if used properly, they can significantly enhance the efficiency with which the minima are located. The input to a minimization program consists of a set of initial coordinates for the system. For the derivative minimization method it is necessary to calculate the derivatives of energy with respect to the variables. Derivatives provide information that can be very useful in energy minimization, and derivatives are used by most popular minimization methods. The direction of the first derivative of the energy indicates where the minimum lies, and the magnitude of the gradient indicates the steepness of the local slope. Moving each atom in response to the force acting on it can lower the energy of the system; the force is equal to minus the gradient. Second derivatives indicate the curvature of the function and predict where the change takes place. The first order minimization methods widely used for the simulations are the steepest descent and conjugate gradient methods.

Steepest Descent will quickly reduce the energy of the structure during the first few iterations. Convergence will slow down considerably as the gradient approaches zero. This method is preferred for systems with large gradients and when the energy is far away from the minimum. Each segment in the steepest descent method tends to reverse progress made

in earlier iteration leading to slower convergence near the minimum. This would require an algorithm that will produce results in conjugate directions and will lead to minimum during successive iteration. Conjugate gradient algorithm does follow the directions and span across the energy surface allowing the minimization to move towards the minimum. This method uses a simple procedure for calculating the new direction vector which is slightly complicated than the steepest descent. This method uses the first derivative in determining the direction for a line search. But additional minimizations have to be performed to make sure the directions are conjugate which can be time consuming since several calculations are performed per iteration.

The new direction vector using the conjugate gradient algorithm can be defined as

$$h_{i+1} = g_{i+1} + \alpha_i h_i \tag{17}$$

Where h_{i+1} is the conjugate gradient, new direction vector from location $i+1$, g_{i+1} is the conjugate gradient at point i+1, h_i is the previous direction and α_i is a constant.

The constant α_i is defined in multiple ways. Using the Polak-Ribiere method the constant is defined as

$$\alpha_i = \frac{(g_{i+1} - g_i) \times g_{i+1}}{g_i \times g_i} \tag{18}$$

Using the Fletcher-Reeves method constant is defined as

$$\alpha_i = \frac{g_{i+1} \times g_{i+1}}{g_i \times g_i} \tag{19}$$

This is a remarkable theorem where the new gradient g_{i+1} is orthogonal to the previous gradients and the new direction h_{i+1} is conjugate with the previous directions. It generates set of orthogonal gradients and conjugate directions. The Fletcher-Reeves method has

lowered the complexity of line minimizations but also the gradient computations. Compared to the steepest descent method it may be longer but it the minimization is more effective with respect to the convergence [77]. A general method to achieve the minimum is typically preferred but it would require more iteration where gradients helps with minimum converge but might require additional computation. This method is more applicable for large systems where storing and changes to the second derivative is required.

Newton Methods require computation and storage of second derivatives and are thus expensive in terms of computer resources. It is used for the systems with maximum of 200 atoms because of the space constraint for storing the second derivative parameters. It has a small convergence radius but it is very efficient near the energy minimum.

Properties Derived from Molecular Simulations

Some of the basic properties like pressure, density can be directly calculated from the ensemble but specific mechanical properties of the structures are determined using the classic technique used in continuum solids. Typically the Young's modulus, bulk modulus and Poisson's ratio are obtained from a tension test. An element is considered to be in stress when an external force is applied on it and when the internal forces try to balance out the external forces applied the body stays in equilibrium. The change in the internal energy of a system with respect to strain per volume constitutes the stress. This strain energy if considered as force applied on a solid surface area then stress can be defined as force acting per unit area. The total internal energy (E_i) can be defined as

$$E^{\alpha} = K^{\alpha} + U^{\alpha} \tag{20}$$

$$K^{\alpha} = \frac{1}{2} M^{\alpha} (v^{\alpha})^2; U_i = \phi^{\alpha}(r) \tag{21}$$

Where $K^{\alpha}, M^{\alpha}, v^{\alpha}$ are the kinetic energy, potential energy and mass of atom α, v^{α} is the velocity magnitude and $\phi^{\alpha}(r)$ is the potential energy at atom location r. Stress contribution can be determined based on the Hamiltonian based on individual energy contributions [78,79]. To determine the Young's modulus, the structure in the stress-free state obtained from MD simulations is subjected to a small amount of strain in the axial direction keeping the other components at zero. With the NVT ensemble the stress contribution to the atomic structure can then be represented as

$$\sigma_{ij} = -\frac{1}{V_0}\left[\sum_{i=1}^{N} m_i v_i v_j^T) + \sum_{i<j} r_{ij} f_{ij}^T\right] \tag{22}$$

Where V_0 is the volume of the system, m_i , v_i, r_{ij}, f_{ij}^T are the mass, velocity, atomic distance and interaction force between the atoms. Typically same equation can be followed for the static model except the first term in the equation removed [80]. The stress calculated is the average stresses of atoms for the volume of the model. The stress calculations are made for every increment in strain by taking the summation of all the atoms. Using MD simulations the results are averaged over time for obtaining the stress- strain curves. Stresses when applied to a system result in change in the atomic positions and the strain tensor can be represented as

$$\varepsilon = \frac{1}{2}\left[(h_0^T)^{-1} G h_0^{-1} - 1\right] \tag{23}$$

Where h_0 represents the matrix formed from vectors a_0, b_0, c_0 , T is the matrix transpose and G is the metric tensor.

When both stress-strain tensors are symmetric the stress and strain can be represented as:

$$\begin{bmatrix} \sigma_{11} & \sigma_{12} & \sigma_{13} \\ \sigma_{21} & \sigma_{22} & \sigma_{23} \\ \sigma_{31} & \sigma_{32} & \sigma_{33} \end{bmatrix} \tag{24}$$

$$\begin{bmatrix} \varepsilon_{11} & \varepsilon_{12} & \varepsilon_{13} \\ \varepsilon_{21} & \varepsilon_{22} & \varepsilon_{23} \\ \varepsilon_{31} & \varepsilon_{32} & \varepsilon_{33} \end{bmatrix} \tag{25}$$

Hooke's law which describes the stress-strain relationship can be written as

$$\sigma_i = C_{ij}\varepsilon_j \tag{26}$$

Where C is elastic stiffness coefficient and is not considered a tensor. And to completely describe the relationship between the behaviors of stress-strain requires a maximum of 21 coefficients.

CHAPTER 4. RESULTS AND DISCUSSION

All simulations were performed using a commercial molecular simulation package Materials Studio from Accelrys Inc. One of the reasons to use this simulation software is it incorporates wide spectrum of molecular mechanics and dynamic methodologies which have shown applicability in molecular modeling. The process and the theory behind the molecular dynamics are explained in detail in Chapter 3. The stress strain behavior of two different composites with varying reinforcement lengths and load applied in longitudinal and transverse directions is studied followed by the effect of varying volume fraction of the reinforcements in the composites is discussed in detail.

Model Building

Two different composites are being examined in this molecular dynamic study. First composite is composed of polyethylene matrix reinforced with CNT which has excellent mechanical and thermal properties and literature has shown the enhancement in the composite properties with the addition of CNTs. The second composite is polyethylene matrix reinforced with GNP and where research documentation on the GNP composites modeling is scarce.

The polymer of interest i.e., polyethylene in this study is modeled to have an amorphous structure. The reason for using polyethylene as a matrix in this study is its simple structure. The polymer C_2H_4 is created using the build tool in the MD package with the chain length and number adjusted with a density of 0.74g/cm3 a shown in Figure 4.1.

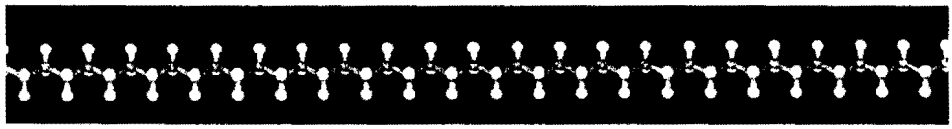

Figure 4.1 Polyethylene chain modeled using material studio simulation package.

Nanotubes and Nanoplatelets structures used as reinforcements for the composites in this study have been modeled along with the polymer structure. Figure 4.2 shows the CNT and GNP structures built using the material studio software.

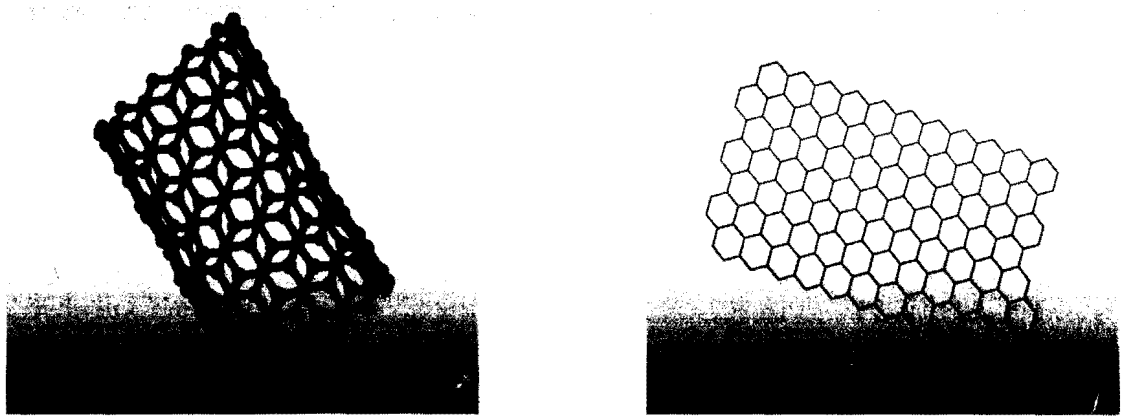

Figure 4.2 Carbon nanotube and nanoplatelet structures modeled in material studio.

When the structures are constructed there is no geometric optimization performed so the structure is minimized to produce a stable conformation. This iterative procedure allows the atom coordinates and possibly the cell parameters to be adjusted so the total energy of the structure is reduced to a minimum. It has been observed that the minimization results in a structural model closely resemble the experimentally observed structure [81]. Structures were minimized using the steepest descent method while the system is far from

an energy minimum point and conjugate gradient when the system was close to a local minimum [82].

The force field used for the simulations is Polymer Consistent Force Field (PCFF) which were parameterized against a wide range of experimental observables and extended to broad range of polymers but the exact parameters for the potential are not available since they are proprietary. In this force field, the interactions within a polymer chain and between polymers chains are described by bonded interactions as well as non-bonded interactions. The bonded interactions include bond-stretching energy, angle bending energy, torsional energy and inversion energy while the non-bonded interactions are vander Waals interactions. The interactions between polymer chains and CNT or GNP are described only by non-bonded interactions. The vander Waals interactions among the polyethylene molecules and between the polymers - CNT/GNP are modeled using Lennard Jones potential. Parameters for the potential were defined for the carbon atoms interaction within the CNT, GNP and ethylene units as σ =0.3825nm and ε =0.4492 kJ/mol [83].

The composites were modeled by inserting the reinforcements into the polyethylene matrix. There is no chemical bonding between the reinforcements and the matrix during the simulation work. Simulations are performed considering vander Waal interactions between the reinforcement and the matrix. A separation distance of 4Å has been maintained between the fillers and the polymer matrix to avoid any repulsive forces. In this study the reinforcements have been modeled at two different lengths termed as long and short CNT/GNPs, to study the effect of the length on the stiffness of the composite. Figure 4.3 shows the long nanotube surrounded by polyethylene matrix.

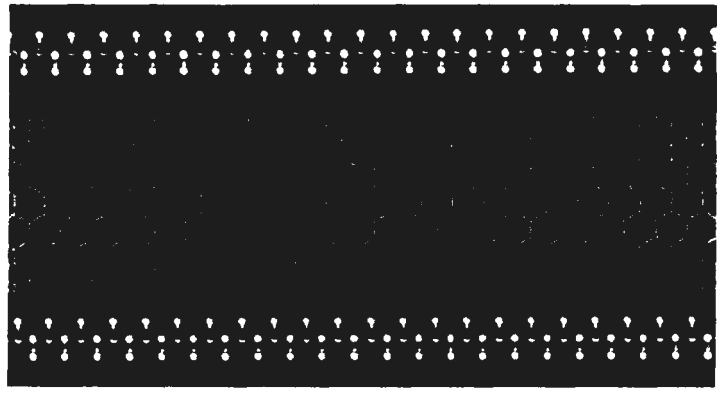

Figure 4.3 Long carbon nanotube surrounded by polyethylene chains.

The long and short (10, 10) CNT was modeled to a length of 45.09Å and 17.32 Å respectively with a diameter of around 11Å. The GNP has thickness of 3.4 Å and was modeled to have two different lengths similar to the CNT. The nanoplatelets are embedded from one end to the other along the longitudinal direction of the cell. A matrix with a 35.8 Å x 35.8 Å x 45.09 Å is constructed and periodic boundary conditions are applied in all directions. In long reinforcement composites the polyethylene matrix contains eight chains of 600 CH2 units and eight chains of 800 CH2 units for the short reinforcement composite. Figures 4.4 and 4.7 show the reinforcements inserted into the polyethylene matrix. The composite had around 14000 atoms in the cell.

After the nanocomposite model is built, the potential energy of the system is likely to be high and not representative of the actual structure. The energy minimization is used to relax such high energy conformations by changing the positions of the atoms in space. Both energy minimization and the MD simulation using NVT ensemble are performed at room temperature. The NVT ensemble keeps constant number of particles, constant volume and temperature and is free to exchange energy. Therefore stresses at different strains can be easily simulated when the different expansions are applied in the longitudinal

and transverse direction of the model. All simulations are run using NVT ensemble at 298K with a 1fs time step. It takes around 24-36 hours for each MD simulation to be run excluding the model building.

Periodic Boundary Condition is used to replicate the cells in all three directions thereby increasing the rigor and realism of the structure. The surface effect is eliminated from the computation by using the boundary conditions, the simulation box replicates throughout the space to form an infinite lattice. When a molecule tends to move in the central box its image in all other boxes moves in the same orientation and the location of the N molecules is measured from the central box.

The elastic properties of the polymer nanocomposites can be obtained by the potential energy change of the structures subject to deformation. Once the stiffness matrix was obtained, the mechanical properties such as Young's modulus can be calculated from the stiffness matrix [84]. In this study, the stiffness matrix was calculated using the constant strain minimization method.

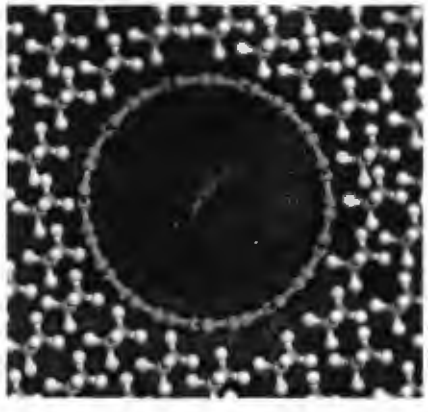

Figure 4.4 Carbon nanotube inserted in the PE matrix.

Simulation Setup

Firstly the normal stress strain curves for the long and the short CNT & GNP composites are studied, when subjected to load in longitudinal and transverse directions with a comparison between composites with different reinforcements.

After the model building the structure load is applied on the periodic cell in longitudinal and transverse directions in increments. For each increment there is a uniform strain that is applied to the entire matrix which means uniformly expanding the cell matrix in the longitudinal and transverse direction and rescaling the new atom coordinates to fit to the new cell dimensions. Figures 4.5 and 4.6 show the direction at which the strain was applied on the cell. The structure is under axial loading when the force is applied along the longitudinal direction.

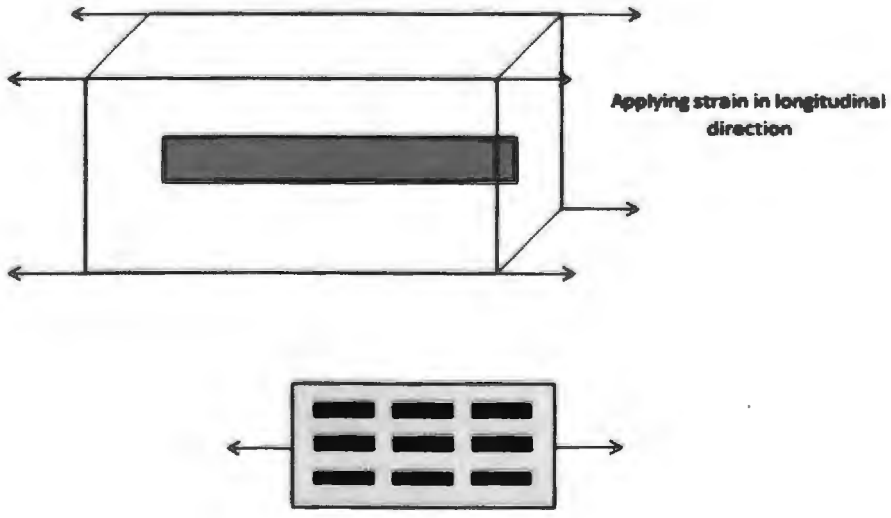

Figure 4.5 Strain applied on the cell in longitudinal direction.

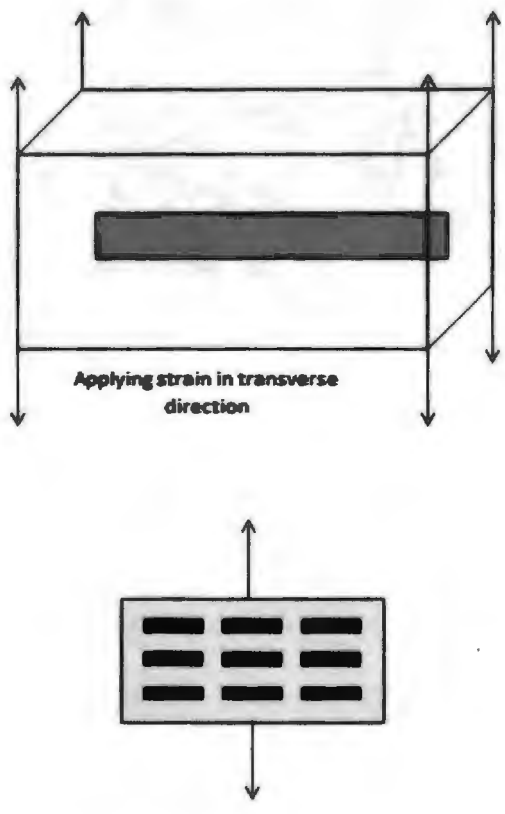

Figure 4.6 Strain applied on the cell in transverse direction.

The MD simulation was continued and the process is repeated for a series of strains up to 10% strain with an increment of 1% in both longitudinal and transverse directions followed by relaxing the structure for around 2ps. The structure is minimized again while keeping the periodic boundary conditions unchanged, and the resultant stress in the minimized structure is calculated from the first derivative of the potential energy with respect to the strain, while the second derivative is the stiffness matrix. The Young's modulus is determined by the inversion of one of the components of the compliance matrix which is obtained by inverting the stiffness matrix.

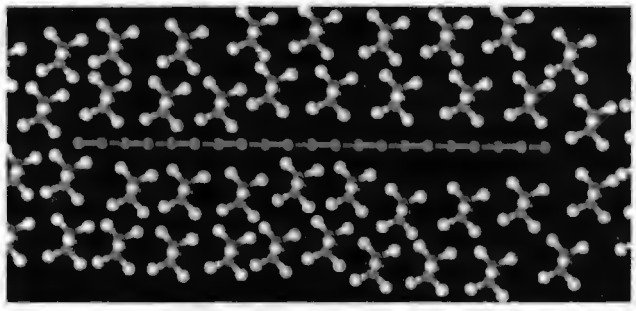

Figure 4.7 GNP inserted in the PE matrix.

Effect of Reinforcement Length on the Composite Stiffness

The computed stress-strain curves of the CNT/GNP-reinforced PE composites in transverse and longitudinal directions are depicted below. Figure 4.8 shows CNT composites behavior when loaded in the transverse direction. The stress-strain curves of long nanotube, short nanotube or without nanotube are close to each other, no enhancement relative to the pure polymer is observed. Therefore, the load in the transverse direction is mainly taken by the PE matrix instead of the nanotube when it is under deformation. Since both the nanotubes occupy the same cross sectional area in the transverse direction no significant difference between the short and long nanotubes was observed.

Similar behavior is observed in case of the GNP composites where the enhancement in composite properties was less than 5%. According to the literature GNPs have the property to enhance stiffness in both directions but the results obtained did not agree with the findings. Further investigation is done to verify if the reinforcement volume has any effect on the properties of the composite. Figure 4.9 shows the PE matrix loaded with nanoplatelets when subjected to transverse loading.

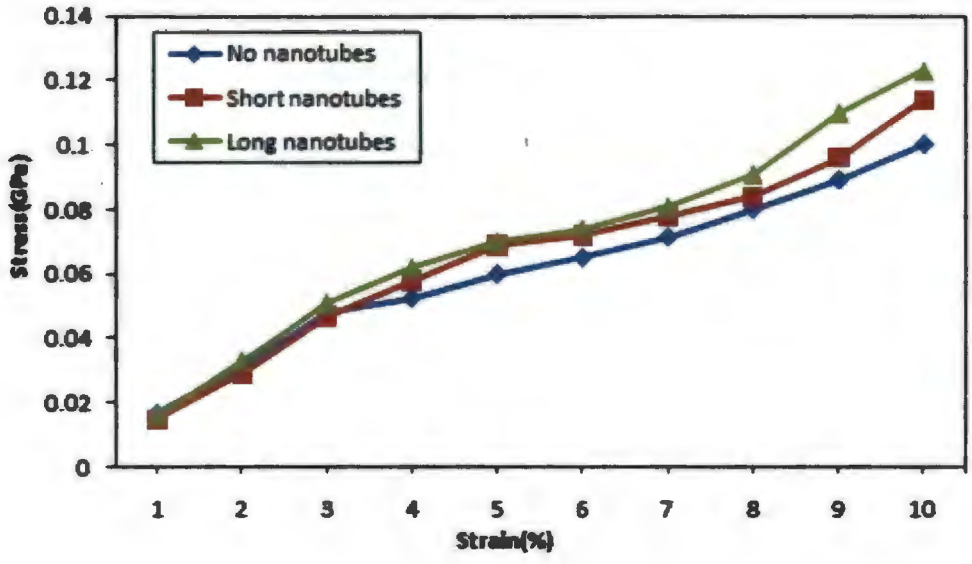

Figure 4.8 Stress vs. Strain curve comparing the long, short and no nanotube polyethylene composites under transverse load.

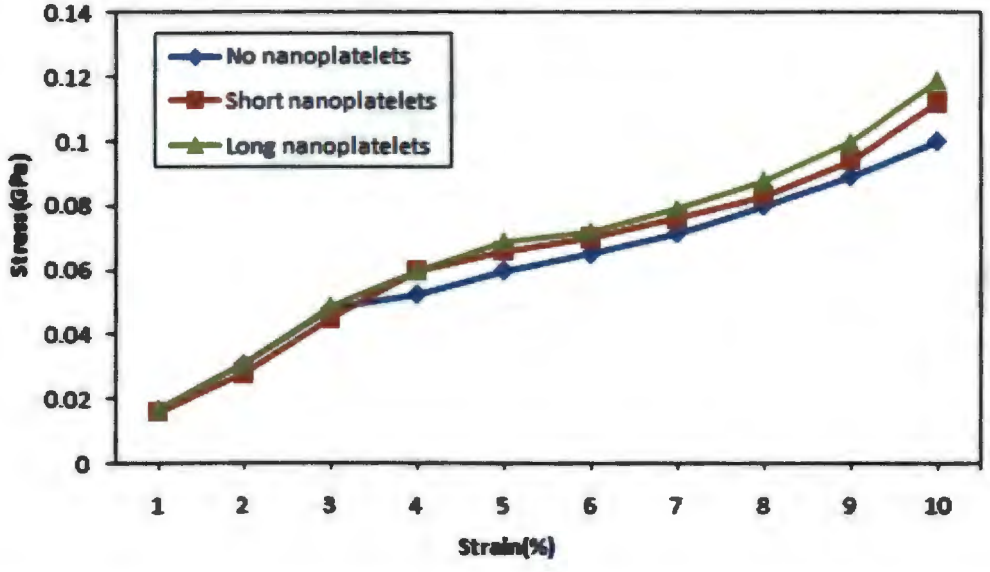

Figure 4.9 Stress vs. Strain curve comparing the long, short and no nanoplatelet polyethylene composites under transverse load.

No significant improvement in the composite stiffness is observed with either reinforcement in the transverse direction. Figure 4.10 shows a comparison between

different composite models. The graphs show that the reinforcement type or the reinforcement length does not have any effect on the stiffness of the composite when the load is applied in the transverse direction. There is limited stress transfer between the polymer and the reinforcement which can be contributed to the weak vander Waal interactions defined between the nanofiller and the polymer in this simulation. Experimental studies might show results different from the modeling since a chemical bond exists between the reinforcement and the polymer leading to load transfer.

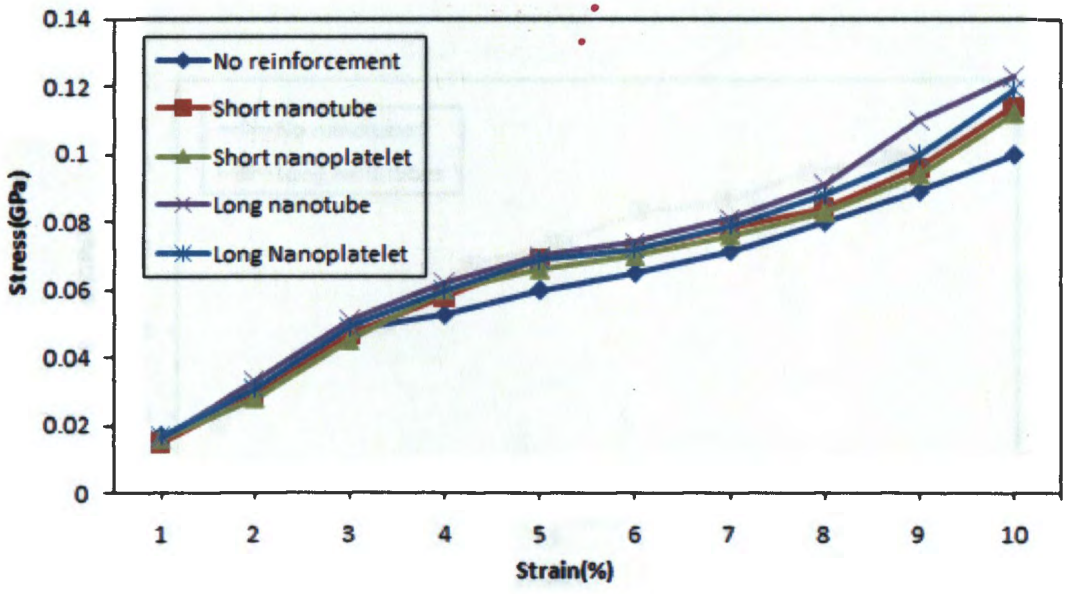

Figure 4.10 Stress vs. Strain curve comparing the nanotube and nanoplatelet polyethylene composites under transverse load.

When the model is subjected to loading in the longitudinal direction there is no enhancement to the polymer using either short nanotube and no nanotube, however, using long nanotube, the stiffness of the PE nanocomposites is greatly improved which is shown in Figure 4.11, which means that the nanotube play an important role in the load transfer in

the longitudinal direction. Figure 4.12 shows that the addition of short nanotube showed little to no improvement in the stiffness which is not surprising and can be attributed to the low aspect ratio of the nanotube in this study compared to the 1:1000 aspect ratio expected from a typical nanotube. Figure 4.13 also shows evidence that the orientation of the polymer along the nanotube axis would allow interfacial adhesion leading to enhancement in the properties. Considering large systems with long nanotubes and polymer chains the structural effects would be larger because of the interactions at a big scale and having a large surface area would allow stronger structural arrangements.

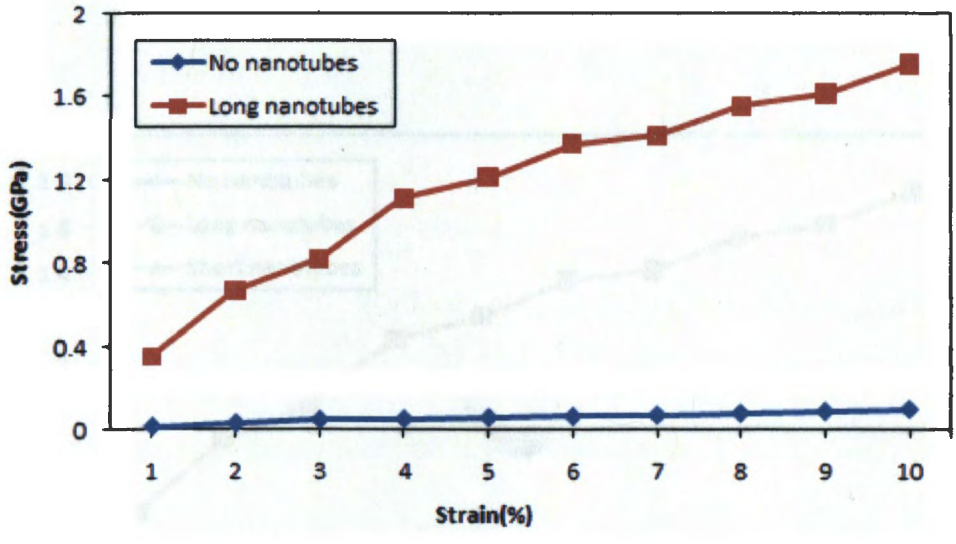

Figure 4.11 Stress vs. Strain curve for the long nanotube composite compared to the no nanotube polyethylene composite under longitudinal load.

The difference in the longitudinal and transverse direction showed that the properties of nanocomposite are not isotropic. The curves from the composites with short nanotube and without nanotubes overlap showing zero enhancement in the properties.

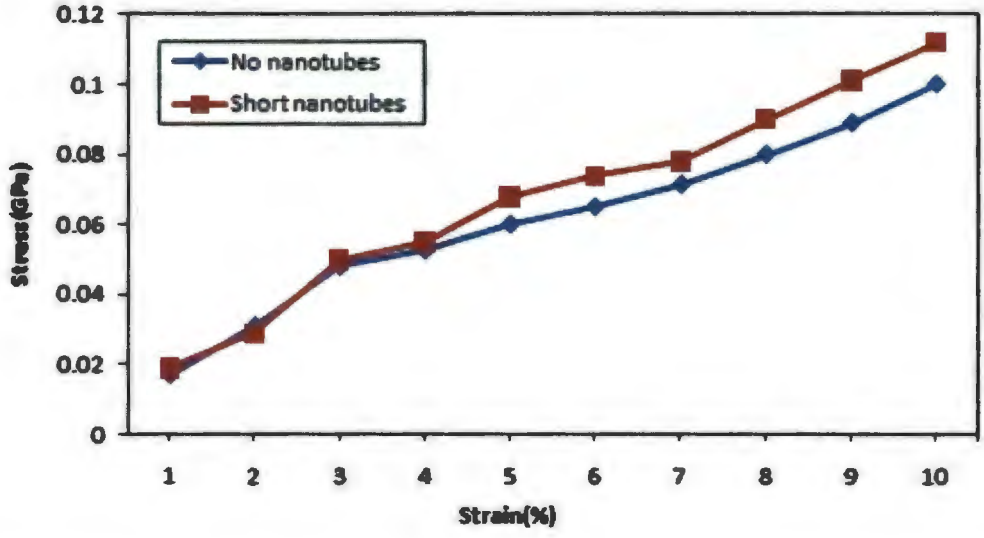

Figure 4.12 Stress vs. Strain curve for the short nanotube composite compared to the no nanotube polyethylene composite under longitudinal load.

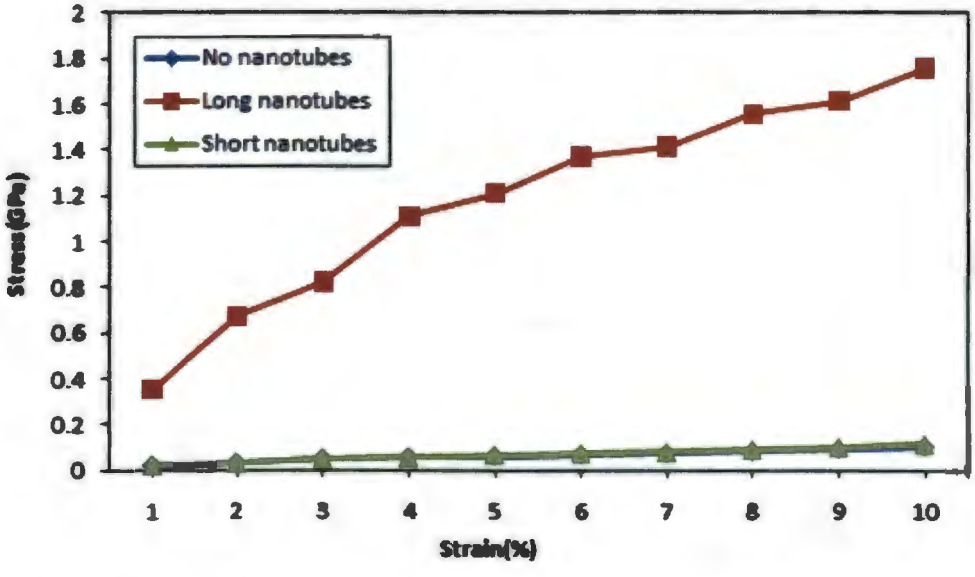

Figure 4.13 Stress vs. Strain curve comparing the long, short, no nanotube polyethylene composites under longitudinal load.

Similar results are observed by using nanoplatelet as reinforcement for PE composites, which is shown in Figures 4.14 and 4.15 in longitudinal direction. The lack of

improvement through the short size reinforcements can be contributed to the weak interactions between the nanofiller and the polymer, no chemical bond existence which would have led to weaker load transfer along with the low aspect ratio is illustrated in Figure 4.16.

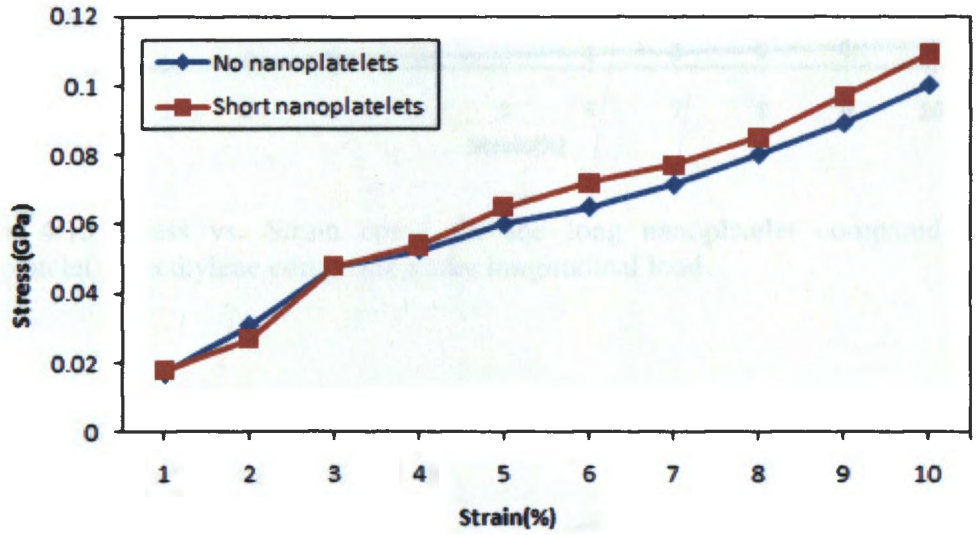

Figure 4.14 Stress vs. Strain curve for the short nanoplatelet composite compared to the no nanoplatelet polyethylene composite under longitudinal load.

A chemical bond between the reinforcement and the polymer has improved the mechanical response as per some studies [84]. The vander Waal interactions are a key contributor towards the mechanical property enhancement of the composites. Graphene nanoplatelets follow a very similar trend as the nanotube under the longitudinal load. A well aligned long polymer chains along the nanotube axis are expected to increase the vander-waal interactions between the polymer and the nanofiller even without a covalent bond between the matrix and the reinforcement.

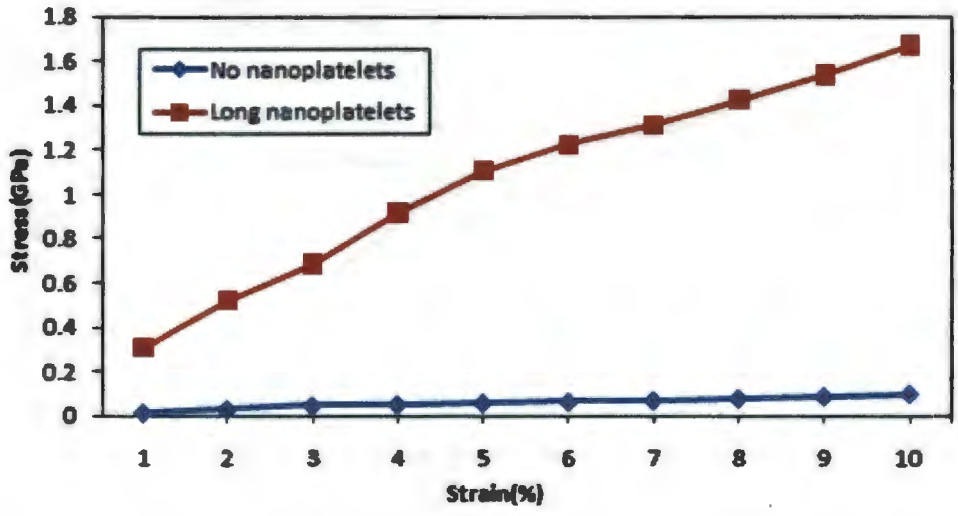

Figure 4.15 Stress vs. Strain curve for the long nanoplatelet compared to the no nanoplatelet polyethylene composite under longitudinal load.

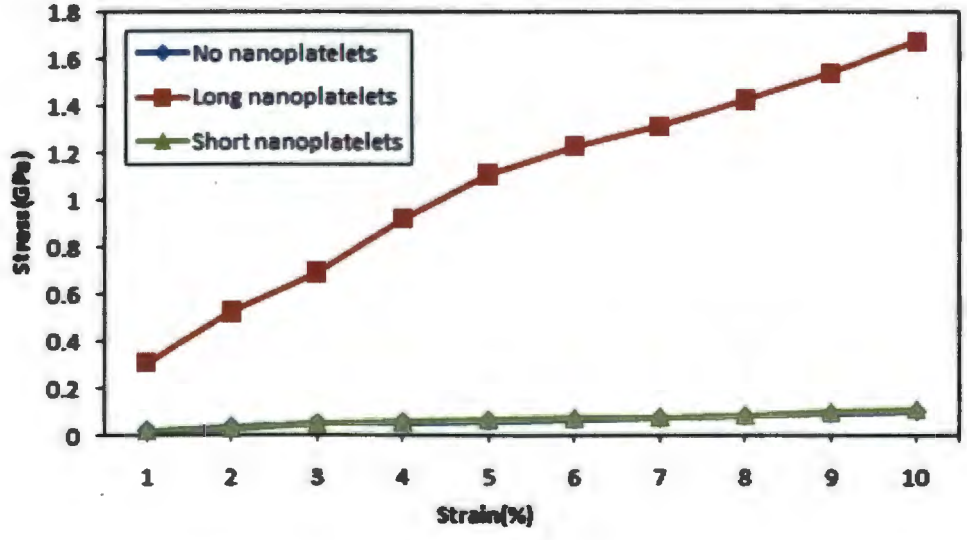

Figure 4.16 Stress vs. Strain curve for the long, short & no nanoplatelet polyethylene composites comparison under longitudinal load.

Comparison of carbon nanotube and graphene nanoplatelet composites properties with long and short reinforcement lengths is illustrated in Figure 4.17.

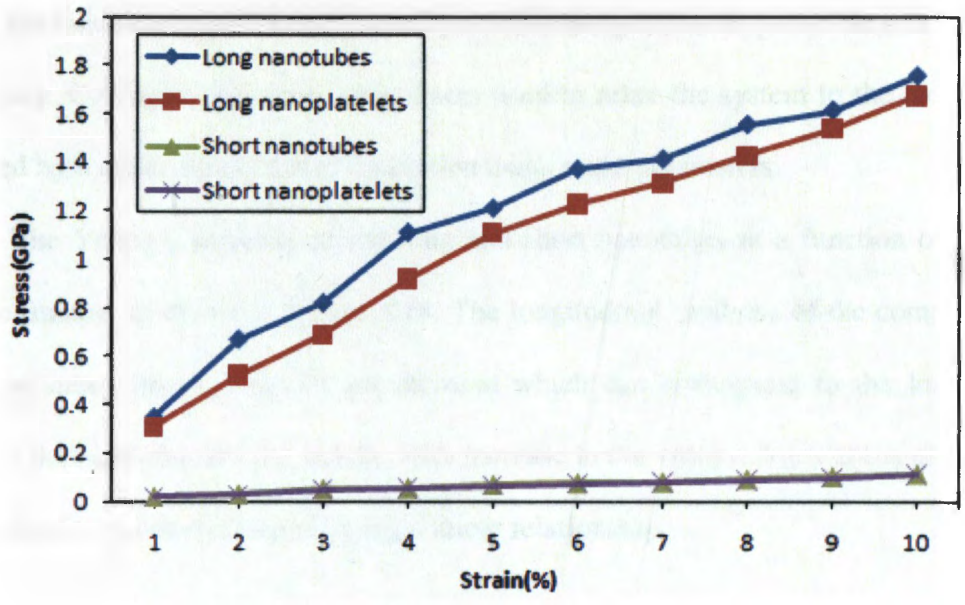

Figure 4.17 Stress vs. Strain curve comparison between nanotube and nanoplatelet polyethylene composites under longitudinal load.

When the CNT composites were compared to the GNP composites the composites with nanotubes were slightly better but not that deferrable which opens doors for utilizing graphene nanoplatelets in various applications. Longer reinforcements in both composites showed around 40% improvement when compared to the shorter reinforcements. The results very well align with the study done by Odegard et al on the carbon nanotube composite simulations [85].

Effect of Reinforcement Volume on the Composite Stiffness

Further investigation has been done to understand the effect the reinforcement volume on the mechanical properties of the two composites. Structures were built with varying volume fractions of reinforcements to study the effect of loading on the properties of the matrix. Volume fractions of the model are calculated as ratio of the filler to the ratio of the matrix. The non-bonded interactions between the reinforcement and the polymer

matrix are modeled using Lennard-Jones potential using the same parameters as mentioned previously. Conjugate Gradient method was used to relax the system to the local minima followed by a molecular dynamic simulation using same parameters.

The Young's modulus of the long and short nanotubes as a function of nanotube volume fraction is shown in Figure 4.18. The longitudinal modulus of the composite with long nanotubes shows a significant increase which can correspond to the load transfer between the nanotube and the matrix, with increase in the volume fraction the efficiency of stress transfer has maximized showing a linear relationship.

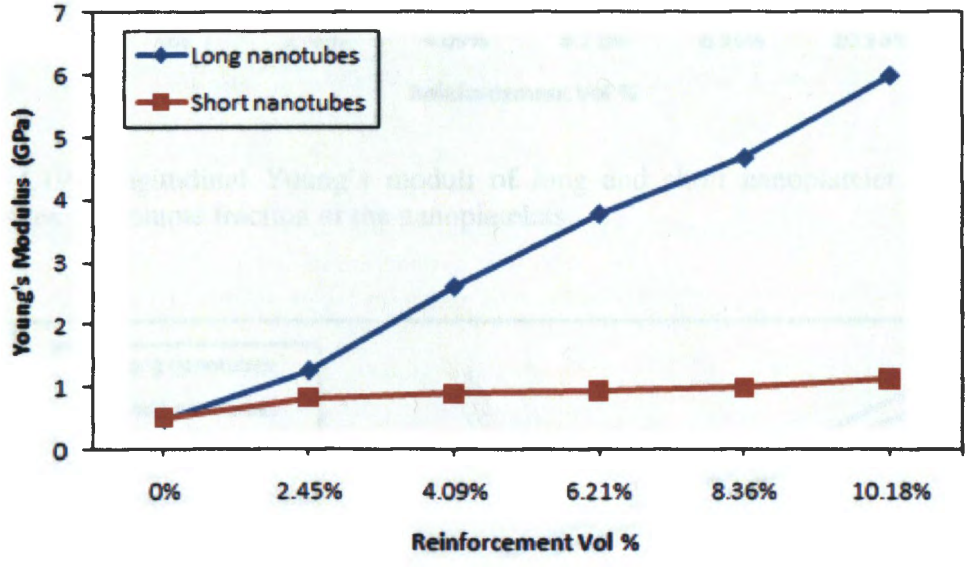

Figure 4.18 Longitudinal Young's moduli of long and short nanotube polyethylene composites vs. nanotube volume fraction.

With the short reinforcement, the curve remained flat showing little to no improvement in the modulus even with the increase in the volume fraction this again can be attributed to the low aspect ratio of the reinforcement and the weak interfacial adhesion as shows in Figure

4.19. The concentration dependence of the Young's modulus calculated in the longitudinal direction, of two polyethylene nanocomposites is shown in Figure 4.20 respectively.

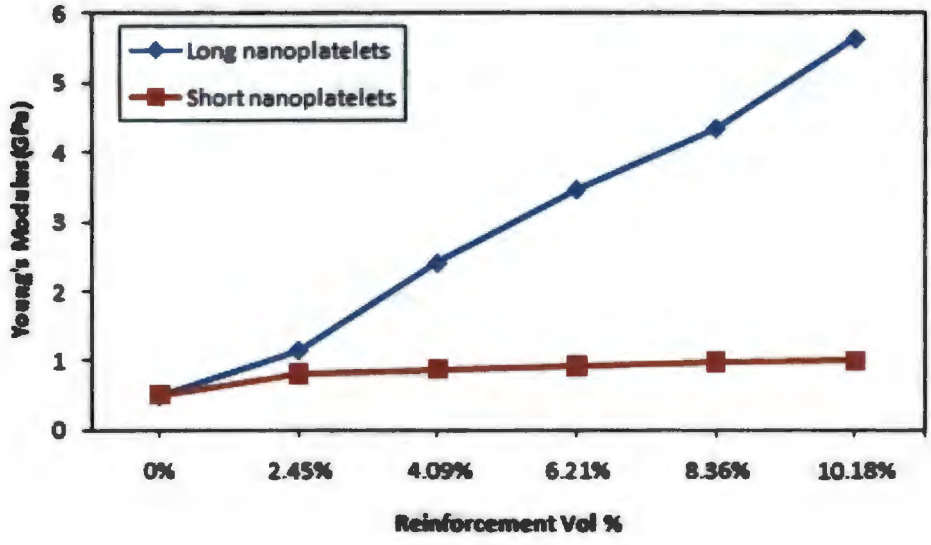

Figure 4.19 Longitudinal Young's moduli of long and short nanoplatelet polyethylene composites vs. volume fraction of the nanoplatelets.

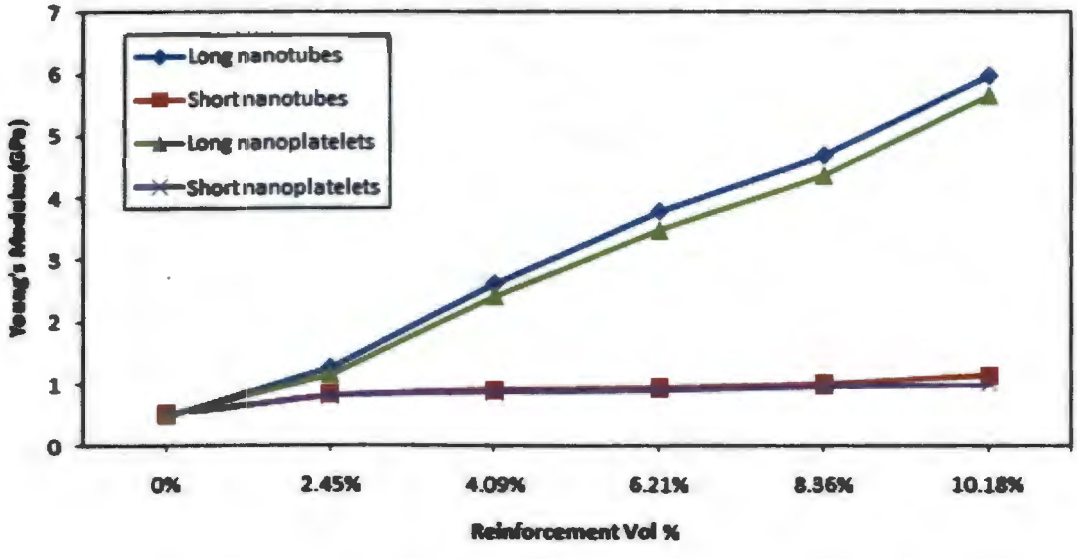

Figure 4.20 Longitudinal Young's moduli comparison of long, short nanotube and nanoplatelet polyethylene composites vs. volume fraction of the reinforcements.

Figure 4.20 clearly shows that moduli increase more or less linearly with increasing reinforcement volume fraction within the range of volume fractions used and that only a small amount of nanofiller can increase the Young's moduli of polyethylene considerably, regardless of the type of reinforcement. In particular, in the case of CNT, the increase in the Young's modulus is higher with the increase in the reinforcement compared to the nanoplatelets. It is obvious that the effect of GNP is not as much as that of CNT. The differences in the mechanical properties of nanoplatelet and nanotube-filled composites may be due to the difference in their aspect ratios and contact surface areas. Compared with GNP, CNT tend to possess a higher aspect ratio at the same volume fraction and filler length and a relatively higher surface area that could interact with the polymer matrix. This explains that the process of exfoliation plays a key role for establishing the bonding between the polymer and the reinforcement for load transfer.

When subjected to transverse loading all the composites with long and short nanotubes and nanoplatelets show modulus in the range of the polymer which means there is no improvement even with the increasing amount of the reinforcement. In this case the type of the reinforcement did not have any effect on the modulus. Figure 4.21 shows the comparison of the different reinforcements at different lengths vs. increasing volume fraction. The most important feature associated with the curve below is the long graphene nanoplatelet composite, transverse modulus was slightly higher compared to the carbon nanotube this can be contributed to the fact that graphene nanoplatelet structure and its large surface area enhances the properties in both directions. Better performance could be obtained by functionalization of the reinforcement with the polymer.

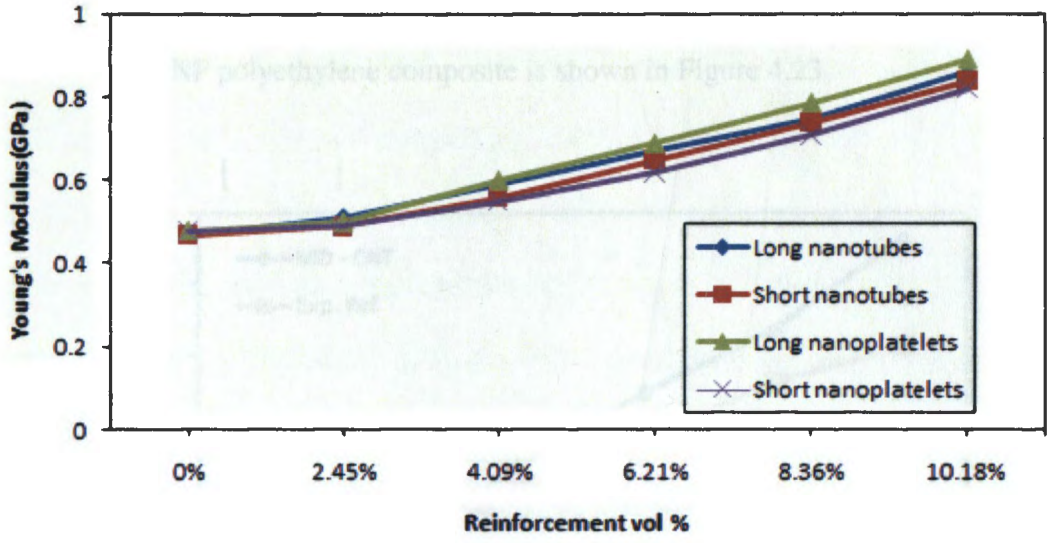

Figure 4.21 Transverse Young's moduli comparison of long and short nanotube and nanoplatelet polyethylene composites vs. volume fraction of the reinforcements.

From the simulation results, it can be said that the length of the reinforcement along with the volume % are a major contributor for mechanical enhancement of the composite and the nanoplatelet reinforced composites do perform equally well when compared to the nanotube composites.

Comparison of Results

The results obtained from the MD simulation above are compared to similar published work [86] and experimental results [87]. Figure 4.22 show the comparison of the results obtained using the MD approach vs. the experimental work for the carbon nanotube polyethylene composite. The disagreement among the results can be attributed to the difference in the aspect ratios, size of the polymer matrix, and alignment of the reinforcement contributing to the difference in the modulus. Molecular structure refinement along with a better forcefield would reduce the gap between the simulation and

experimental work. The comparison of the published results with the results obtained on the CNT and GNP polyethylene composite is shown in Figure 4.23.

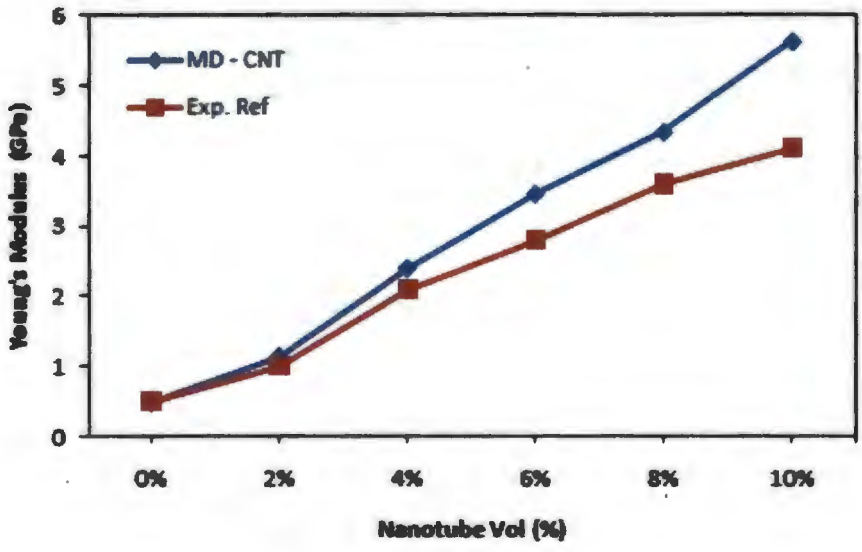

Figure 4.22 Comparison of Young's moduli obtained from the molecular dynamic simulation and experimental data of carbon nanotube polyethylene composite.

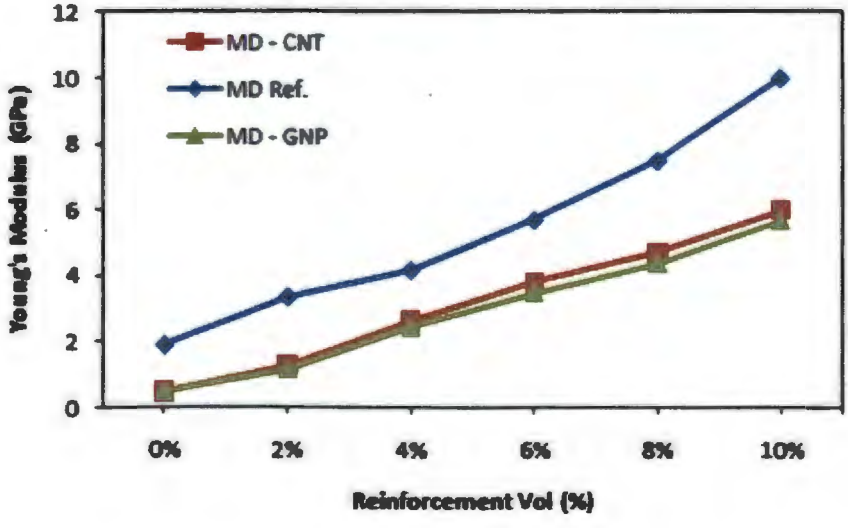

Figure 4.23 Comparison of Young's moduli of carbon nanotube and graphene nanoplatelet polyethylene composite obtained from our research and published results.

The big difference in the modulus can be attributed to the systems being compared and the variations due to the different modeling approaches. The reference is a MD study based on Brenner's potential and is performed using DL Poly software package. The aspect ratios and the matrix size in the reference is twice that of ours, the shortest reinforcement length being 6nm. And this explains the higher young's modulus values seen with the increase in the reinforcement volume. This comparison is carried out since similar methodologies and techniques were used for calculating the modulus of the composite. Though the values are different but the trend of enhancement in the composite properties is in close agreement.

CHAPTER 5. CONCLUSIONS AND RECOMMENDATIONS

In this thesis, two different composite models, nanotube and nanoplatelet polymer composites have been introduced and the fundamental understanding of interface along with the mechanical properties is studied. Molecular dynamic simulation approach was utilized to study the systems. Theory behind the simulation work along with the parameters used in building the structures, setup with the procedures was discussed in detail. Comparison was made between the nanotube and nanoplatelet PE composite properties to verify if the GNP can serve as an alternative material, which can be produced more cost effectively in comparison to CNTs.

A unit strain was applied on the nanotube and nanoplatelet composite periodic cell and using the stress strain curves the effect of the reinforcement length on the composite properties were studied. The results were evaluated and the simulation shows that the stiffness of the composite increases with increase in the reinforcement length when composites were subjected to longitudinal loads. There was significant load transfer between the reinforcement and the polymer in the longitudinal direction for the longer reinforcements. The shorter reinforcements when loaded in either direction showed no improvement which contributes to its low aspect ratio. But little to no improvement was observed when the load was applied on the cell in the transverse direction irrespective of the reinforcement length. This proves that the nanocomposites are not isotropic and it has much greater strength in the longitudinal direction compared to the transverse direction. The nanotube and nanoplatelet composites properties were pretty comparable and composites with nanotubes had stiffness around 10% better than the nanoplatelet reinforced

composites. Because of the relatively low aspect ratio and surface area of nanoplatelet compared with nanotube, the strength increase of using nanotube as filler is higher than that of using nanoplatelet; however, nanoplatelet is much easier to be synthesized than nanotube.

Further work was done to study the effect of reinforcement volume on the mechanical properties of composites loaded with nanotubes and nanoplatelets in longitudinal and transverse directions. The Young's modulus values were generated from the stress strain curves and as expected the strength of the composite increased with increasing volume of the reinforcement in the longitudinal direction for long reinforcements by more than 40%. Even though the reinforcement volume was increased, the shorter nanofillers did not show any improvements in the properties which can be accounted for the vander-waal interactions between the reinforcement and the polymer. Similar behavior was observed with the composites loaded under transverse direction but the long nanoplatelet composite under transverse load showed slight improvement in the strength from 6.21% reinforcement volume proving that their structure can enhance the properties in both directions. The results well align with some of the studies that have been done in the molecular dynamic simulation field. Overall study proves that the nanoplatelet reinforced composite properties are not much deferrable compared to the nanotube composites and the MD simulations is an effective tool that can be used for studying the properties of materials at much lower cost compared to experimental studies.

Suggestions for Future Work

The major area for future work can be to study the interface between the nanofillers

and the polymer by introducing a covalent bond between them and analyzing its impact on the polymer properties. It is very challenging and complicated to model a structure with chemical bonding links designed for effective load transfer. This study can help reduce the gaps that currently exist between the experimental versus computational studies. Another important factor can be to determine the ideal length of the reinforcement that is required for any enhancement in the polymer properties since studies have always proven that the shorter nanofillers do not have the load transfer capability.

Further investigation on the orientation of reinforcement in the matrix, the geometric arrangement can be done to study its impact on the properties of the composite. The structure of the polymer also has an effect on its interfacial interactions with the nanofiller; a more cross linked polymer chain can have stronger interactions compared to a simple polymer resin, investigating composites with different polymer matrix materials can lead to several new facts. These simulation modeling techniques can also be utilized to determine other composite properties like dynamic response, impact toughness, thermal and electrical conductivities etc. Molecular structures obtained from the MD simulations can also be used as an input for equivalent-continuum modeling technique for determining the bulk properties of composites.

REFERENCES

1. Endo, K., Koizumi, T., Otsuka, T., Analysis of electron spectra of carbon allotropes by density functional theory calculations using the model molecules, *Journal of Physical Chemistry*, 2003, 107, 9403-9408.
2. Haddon, R.C., Magnetism of the carbon allotropes, *Nature*, 1995, 378, 249-255.
3. Griffith, A.A., The theory of rapture, *Proceedings of the First International Congress on Applied Mechanics*, 1924, 55.
4. Gordon, J.E., The new science of strong material, *Princeton Universal Press*, 1984.
5. Griffith, A.A., The phenomena of rapture and flaw in solids, *Philosophical Transactions of the Royal Society of London*, 1920, A221, 163-198.
6. Prasad, D., Jemmis, E., Stuffing improves the stability of fullerene like boron clusters, *Physical Review Letters*, 2008, 100, 165504-165507.
7. Smalley, R., Discovering the fullerenes, *Reviews of Modern Physics*, 1997, 69, 723-730.
8. Wardman, R., For carbon, it's a whole new ball game, *The Helix*, 1991, 24, 14-15.
9. Bacon, R., Growth, structure, and properties of graphite whiskers, *Journal of Applied Physics*, 1960, 31, 283-290.
10. Bianconi, P., et al., Diamond and diamond like carbon from a pre-ceramic polymer, *Journal of American chemical society*, 2004, 126, 3191-3202.
11. Iijima, S., Helical microtubules of graphitic carbon, *Nature*, 1981, 354, 56-58.
12. Esfarjani, K., Electronic and transport properties of N-P doped nanotubes, *Applied Physics Letters*, 1999, 74, 79-81.

13. Baker, R.K., Rodriguez, N.M., Crystalline graphite nanofibers and a process for producing same, *Catalytic Materials LLC*, 2003.

14. Kolotilo, D.M., Chemical bond and properties of graphite materials, *Powder Metallurgy and Metal Ceramics*, 1968, 7, 966-971.

15. Gao, G., Cagin, T., Goddard, W.A., Energetics, structure, thermodynamic and mechanical properties of nanotubes, *Nanotechnology*, 1998, 9, 183-191.

16. Collins, P.G., Avouris, P., Nanotubes for electronics, *Scientific American*, 2000, 283, 62-69.

17. Harris, P.J.F., Carbon nanotubes and related structures – New materials for the twenty-first century, *ChemPhysChem*, 2002, 3, 463-464.

18. Tagmatarchis, N., Prato, M., Carbon based materials: From fullerene nanostructures to functionalized carbon nanotubes, *Pure Application Chemistry*, 2005, 77, 1675-1684.

19. Mintmire, J.W., White, C.T., Electronic and structural properties of carbon nanotube, *Carbon*, 1995, 33, 893-902

20. Thess, A., Lee, R., Nikolaev, P., Robert, J., Fischer, J.E., Crystalline ropes of metallic carbon nanotubes, *Science*, 1996, 273, 483.

21. Lyshevski, M.A., Carbon nanotube analysis, classification and characterization, *Nanotechnology, 4th IEEE Conference*, 2004, 527-529.

22. Robertson, D.H., Brenner, D.W., Mintmire, J.W., Energetics of nanoscale graphitic tubules, *Physical Review B*, 1992, 45, 12592.

23. Endo, M., Saito, R., Dresselhaus, M.S., Ebbesen, T.W., Carbon nanotubes: Preparation and properties, *CRC Press*, Boca Raton, 1997, 5, 35-110.

24. Milewski, J.V., Katz, H.D., Handbook of fillers for plastics, *Van Nostrand Reinold Company*, 1987, 42, 14-33.

25. Sinnott, S.B., Andrews, R., Carbon nanotubes: Synthesis, properties, and applications, *Critical Reviews in Solid State and Material Sciences*, 2001, 26, 145-249.

26. Lee, C., Wei, X., Kysar, J.W., Hone, J., Measurement of the elastic properties and intrinsic strength of monolayer graphene, *Science*, 2008, 321, 385-388.

27. Currie, L.M., Hamister, V.C., MacPherson, H.G., The production and properties of graphite for reactors, *National Carbon Company*,1955.

28. Zheng, W.G., Wong, S.C., Electrical conductivity and dielectric properties PMMA/expanded graphite composites, *Composites Science and Technology*, 2003, 63, 225-235.

29. Zheng, W.G., Lu, X.H., Wong, S.C., Electrical and mechanical properties of expanded graphite - reinforced high density polyethylene, *Journal of Applied Polymer Science*, 2004, 91, 2781-2788.

30. Cerezo, F.T., Preston, C.M.L., Shanks, R.A., Structural, mechanical and dielectric properties of poly (ethylene-co-methul acrylate-co-acryclic acid) graphite oxide nanocomposites, *Composites Science and Technology*, 2007, 67, 79-91.

31. Dresselhaus, M.S., Dresselhaus, G., Intercalation compounds of graphite, *Advances in Physics*, 1981, 30, 139.

32. Zheng, W., Lu, X., Wong, S.C., Electrical and mechanical properties of expanded graphite-reinforced high density polyethylene, *Journal of Applied Polymer Science*, 2004, 91, 2781-2788.

33. Eizenberg, M., Blakely, J.M., Carbon monolayer phase condensation on Ni, *Surf. Sci.*, 1970, 82, 228-236.

34. Novoselov, K.S., Geim, A.K., Morozov, S.V., Jiang, D., Dubonos, S.V., Firsov, A.A., Electric field effect in atomically thin carbon films, *Science*, 2004, 306, 666-669.

35. Karmakar, S., Kulkarni, N.V., Nawale, A.B., Lalla, N.P., Mishra, R., Sathe, V.G., Bhoraskar, S.V., Das, A.K., A novel approach towards selective bulk synthesis of few-layer graphenes in an electric arc, *Journal of Physics*, 2009, 42, 115201/1 – 115201/14.

36. Tsai, J.L., Chen, C.W., Characterizing mechanical properties of graphite nanoplatelets, *17th American society of Composites Annual Conference*, 2002.

37. Kalaitzidou, K., Fukushima, H., Askeland, P., Drzal, L.T., The nucleating effect of exfoliated graphite nanoplatelets and their influence on the chemical structure and electrical conductivity of polypropylene nanocomposites, *Journal of Material Science*, 2008, 43, 2895-2907.

38. Wong, S.C., Wouterson, E.M., Sutherland, E.M., Dielectric properties of graphite nanocomposites, *In proceedings of the 63rd Annual Technical Conference of the Society of Plastic Engineers*, Boston, U.S.A., ANTEC,2005.

39. Wang, S., Tambraparni, M., Qiu, J., Tipton, J., Dean, D., Alternate multilayer films of poly(vinyl alcohol) and exfoliated graphene oxide fabricated via a facial layer-by-layer assembly, *Macro-molecules*, 2009, 42, 5251-5255.

40. Lee, C., Wei, X., Kysar, J.W., Hone, J., Measurement of the elastic properties and intrinsic strength of monolayer graphene, *Science*, 2008, 321, 385-388.

41. Ramanathan, T., Abdalla, A.A., Stankovich, S., Dikin, D.A., Herrera-Alonso, M., Piner, R.D., Adamson, D.H., Schniepp, H.C., Chen, X., Ruoff, R.S., Nguyen, S.T.,

Aksay, I.A., Brinson, L.C., Functionalized graphene sheets for polymer nanocomposites, *Nature Nanotechnology*, 2008, 3, 327-331.

42. Kim, H., Miura, Y., Macosko, C.W., Graphene/ Polyurethane nanocomposites for improved gas barrier and electrical conductivity, *Chemistry of Materials*, 2010, 22, 3441-3450.
43. Odegard, G.M., Gates, T.S., Modeling and testing of graphite nanoplatelet/epoxy composite, *Journal of Intelligent Material Systems and Structures*, 2006, 17, 239–246.
44. Gersappe, D., Molecular mechanisms of failure in polymer nanocomposites, *Physical Review Letters*, 2002, 89, 058301, 1-4.
45. Vollenberg, P.H.T., Heikens, D., Particle size dependence of the Young's modulus of filled polymers: 1. Preliminary Experiments, *Polymer*, 1989, 30, 1656-1662.
46. Brechet, Y., Cavaille, J.Y.Y., Chabert, E., Chazeau, L., Dendievel, R., Flandin, L., Gauthier, C., Polymer based nanocomposites: Effect of filler-filler and filler matrix interactions, *Advanced Engineering Materials*, 2001, 3, 571-578.
47. Piggott, M.R., Load bearing fiber composites, *Pergamon Press*, 1980, 69-71.
48. Shia, D., Hui, C.Y., Burnside , S.D., Giannelis, E.P., An interface model for the prediction of young's modulus of layered silicate-elastomer nanocomposites, *Polymer Composites*, 1998, 19, 608-617.
49. Sato, N., Kurauchi, T., Sato, S., Kamigaito, O., SEM observations of the initiation and propagation of cracks in a short fiber reinforced thermoplastic composite under stress, *Journal of Material Science Letters*, 1983, 2, 188-190.
50. Sato, N., Kurauchi, T., Sato, S., Kamigaito, O., Reinforcing mechanism of small diameter fiber in short fiber composite, *Journal of Composites*, 1988, 22, 850-873.

51. Nardin, M., Schultz, J., Interactions and properties of composites: Fiber matrix adhesion measurements in the interfacial interactions in polymeric composites, *Kluwer Academic Publishers*, 1993, 81-92.

52. Feng, X.Q., Huang, Y., Hwang, K.C., Micro and nano-mechanics of carbon nanotubes composites, *21st International Congress of Theoretical and Applied Mechanics, Conference proceedings*, Warsaw, Poland, 2004.

53. Griebel, M., Hamaekers, J., Molecular dynamics simulations of the elastic moduli of polymer-carbon nanotube composites, *Computer Methods in Applied Mechanics and Engineering*, 2004, 193, 1773-1788.

54. Frankland, S.J.V., Caglar, A., Brenner, D.W., and Griebel, M., Molecular simulation of the influence of chemical cross-links on the shear strength of carbon nanotube – polymer interfaces, *Journal of Physical chemistry*, 2002, 106, 3046-3048.

55. Wang, Y., Ju, S., Cheng, H., Lu, J., Wang, H., Modeling of polyethylene and functionalized CNT composites: A dissipative particle dynamics study, *Journal of Physical Chemistry*, 2010, 114, 3376-3384.

56. Odegard, G.M., Gates, T.S., Wise, K.E., Park, C., and Siochi, E.J., Constitutive modeling of nanotube-reinforced polymer composites, *Composite Science Technology*, 2003, 63, 1671-1681.

57. Han, Y., Elliott, J., Molecular dynamics simulations of the elastic properties of polymer/carbon nanotube composites, *Computational Material Science*, 2007, 39, 315-323.

58. Cadek, M., Coleman, J.N., Barron, V., Hedicke, K., Blau, W,J., Morphological and mechanical properties of carbon-nanotube-reinforced semicrystalline and amorphous polymer composites, *Applied Physics Letter*, 2002, 81, 5123-5125.

59. Tallury, S., Pasquinelli, M., Molecular dynamics simulations of flexible polymer chains wrapping single-walled carbon nanotubes, *Journal of Physics*, Chem. B, 2010, 114, 4122- 4129.

60. Li, L., Xia, Z.H., Curtin, W.A., Yang, Y.Q., Molecular dynamics simulations of interfacial sliding in carbon nanotube/diamond nanocomposites, *Journal of the American Ceramic Society*, 2009, 92, 2331-2336.

61. Ruoff, R.S., Stankovich, S., Piner, R.D., Nguyen, S.T., Synthesis and exfoliation of isocyanate treated grapheme oxide nanoplatelets, *Carbon*, 2006, 44, 3342-3347.

62. Vadim, V.S., Computational and experimental mechanics of advance materials, *CISM International Center for Mechanical Sciences*, 2010, 7, 259.

63. Frenkel, D., Smit, B., Understanding molecular simulation: From algorithms to applications, *Academic press*, 2002.

64. Alder, B.J., Wainwright, T.E., Studies in molecular dynamics, *The Journal of Chemical Physics*, 1957, 27, 1208-1209.

65. Rahman A., Correlations in the motion of atoms in liquid argon, *Physics Revision*, 1964, 136, 405.

66. Born, M., Oppenheimer, R., Zur Quantentheorie der Molekeln, *Annals of Physics*, 1927, 84, 457-484.

67. Verlet, L., Computer "experiments" on classical fluids. I. thermodynamical properties of lennard- jones molecules, P*hysical Review*, 1967, 159, 98-103.

68. Maple, J.R., Dinur, U., Hagler, A.T., Derivation of force fields for molecular mechanics and dynamics from ab initio energy surfaces, *Proc. Natl. Acad. Sci*, 1988, 85, 5350.

69. Mac, K., All - atom empirical potential for molecular modeling and dynamics studies of proteins, *Journal of Physics, Chem. B*, 1998, 102, 3586-3616.

70. Huai, S., Mumby, S.J., Maple, J.R., Hagler, A.T., An ab initio CFF93 all-atom force field for polycarbonates, *Journal of the American Chemical Society*, 1994, 116, 2978-2987.

71. Sun, K., Adaptive motion estimation based on statistical sum of absolute difference, *IEEE International Conference on Imagine Processing*, 1998, 3, 601-604.

72. Nose, S., A unified formulation of the constant temperature molecular dynamics methods, *Journal of Chemical Physics*, 1984, 81, 511-519.

73. Hoover, W.G., Canonical dynamics: Equilibrium phase - space distributions, *Physical Review A*, 1984, 31, 1695-1697.

74. Brendsen, H.J., Postma, J.P.M., Gunsteren, W.F.V., Nola, A.D., Haak, J.R., Molecular dynamics with coupling to an external bath, *Journal of Chemical Physics*, 1984, 81, 3684-3690.

75. Makov, G., Payne, C.M., Periodic boundary conditions in ab initio calculations, *Physics*, 1995, 51, 4014-4022.

76. Catlow, C.R.A., Energy minimization techniques in materials modeling, *Handbook of Materials Modeling*, 2005, 2, 547-564.

77. Parrinello, M., Rahman, A., Polymorphic transitions in single crystals: A new molecular dynamics method, *Journal of Applied Physics*, 1981, 52, 7182-7190.

78. Vitek, V., Egami, T., Atomic level stresses in solids and liquids, *Physica Status Solidi*, 1987, 144, 145-156.

79. Nielsen, O.H., Martin, R.M., Stresses in semiconductors: Ab initio calculations on Si, Ge and GaAs, *Physics*, 1985, 32, 3792-3805.

80. Theodorou, D.N., Boone, T.D., Dodd, L.R., Mansfield, K.F., Stress tensor in model polymer systems with periodic boundaries, *Macromolecular Theory and Simulations*, 1993, 2, 191-238.

81. Walton, E.B., Van Vliet, K.J., Equilibration of experimentally determined protein structures for molecular dynamics simulation, *Physical Review*, 2006, 74, 061901.

82. Spyriouni, T., Vergelati, C., A molecular modeling study of binary blend compatibility of polyamide 6 and poly vinyl acetate with different degrees of hydrolysis: An atomistic and mesoscopic approach, *Macromolecules*, 2001, 34, 5306-5316.

83. Clarke, J.H.R., Binder, K., Monte Carlo and molecular dynamics in polymer sciences, *Oxford University Press*, 1995, 272.

84. Odegard, G.M., Clancy, T.C., Gates, T.S., Modeling of the mechanical properties of nanoparticle/polymer composites, *Polymer*, 2005, 46, 553-562.

85. Frankland, S.J.V., Harik, V.M., Odegard, G.M., Gates, T.S., Constitutive modeling of nanotube –reinforced polymer composites, *Composites Science and Technology*, 2003, 63, 1671-1687.

86. Odegard, G.M., Frankland, S.J.V., Gates, T.S., The effect of chemical functionalization on mechanical properties of nanotube/polymer composites, *AIAA Journal*, 2005, 43, 1828-1835.

87. Haggenmueller, R., Zhou, W., Fischer, J.E., Winey, K.I., Production and characterization of polymer nanocomposites with highly aligned single-walled carbon nanotubes, *Journal of Nanoscience and Nanotechnology*, 2003, 3, 105-110.